NPS ARCHIVE
1969
NILSEN, T.

COMMUTATED NETWORK FILTER

by

Tor Rønholt Nilsen

United States
Naval Postgraduate School

THESIS

COMMUTATED NETWORK FILTER

by

Tor Rønholt Nilsen

December 1969

This document has been approved for public release and sale; its distribution is unlimited.

Library
U.S. Naval Postgraduate School
Monterey, California 93940

Commutated Network Filter

by

Tor Rønholt Nilsen
Lieutenant Commander, Royal Norwegian Navy

Submitted in partial fulfillment of the
requirements of the degree of

MASTER OF SCIENCE IN ELECTRICAL ENGINEERING

from the

NAVAL POSTGRADUATE SCHOOL
December 1969

NPS Archive
1969
Nissen, T.

Thesis N59 c.1

ABSTRACT

This thesis presents the results obtained in computer simulations of the commutated network filter. The commutated network filter is also used as a bandpass filter in servosystems. A linear approximation to the transfer function is found to be usable for design purposes.

Library
U.S. Naval Postgraduate School
Monterey, California 93940

TABLE OF CONTENTS

I. INTRODUCTION 11

II. COMMUTATED NETWORK CONFIGURATIONS AND COMPUTER SIMULATIONS OF THE NETWORK 12

III. FREQUENCY RESPONSE OF FILTER 21

IV. APPLICATION OF FILTER IN SERVOSYSTEMS 24

V. APPROXIMATION OF FILTER TRANSFER FUNCTION 34

VI. CONCLUSION 37

APPENDIX A - Time Responses of Servosystem 38

LIST OF REFERENCES 55

INITIAL DISTRIBUTION LIST 56

FORM DD 1473 57

LIST OF TABLES

I	Fourier coefficients of output signal Y	20
II	Results of frequency response simulation - phase	23
III	Values used for computer simulation	39

LIST OF ILLUSTRATIONS

2.1	Commutated capacitor	12
2.2	Coupled commutated network	12
2.3	Uncoupled commutated network	13
2.4	Equivalent circuit of commutated networks	13
2.5	Four-capacitor commutated network	13
2.6	Equivalent circuit for figure 2.5	14
2.7	Computer program for simulation	14
2.8	Square-wave F	15
2.9	Square-wave P	15
2.10	Commutating square-waves	16
2.11	Filter configuration	17
2.12	Computer program for Fourier analysis	19
3.1	Frequency response of filter - (phase)	22
4.1	Servosystem of example 1	24
4.2	Compensated filter network	25
4.3	Bode-plot of system of figure 4.1	26
4.4	Time response to unit step input.KMO=8.636×10^{11}	28
4.5	Time response to unit step input.KMO=2.0×10^{12}	29
4.6	Time response to unit step input.KMO=2.5×10^{12}	30
4.7	Bode-plot for example 2	31
4.8	Bode-plot for example 3	32
4.9	Bode-plot for example 4	33
5.1	Poles and zeros of T(s)	34
5.2	Bode-plot for T(s) and computer results for CN	36

A.1 Values used for time responses 38

A.2-A.16 Time responses to unit step input 40-54

ACKNOWLEDGEMENT

Appreciation for the encouragement and guidance rendered by Dr. G. J. Thaler of the Naval Postgraduate School during the preparation of this thesis is hereby gratefully expressed.

I. INTRODUCTION

A commutated network is an electrical network, either active or passive, consisting of resistors and reactive elements which are switched or commutated in a periodic manner. In most practical cases the reactive elements are capacitors. There are several configurations of a commutated network used in the field of electrical engineering. The configuration used here is that of commutated capacitors used in the feed-back path around an operational amplifier. Thus by applying commutation action to the capacitors in a lag network, the low-pass frequency response of that network can be transformed into that of a highly selective bandpass filter. The center frequency of the bandpass characteristic will be the same as the commutation frequency.

II. COMMUTATED NETWORK CONFIGURATION AND COMPUTER SIMULATIONS OF THE NETWORK

The fundamental element of commutated networks is the capacitor shown in fig. 2.1.

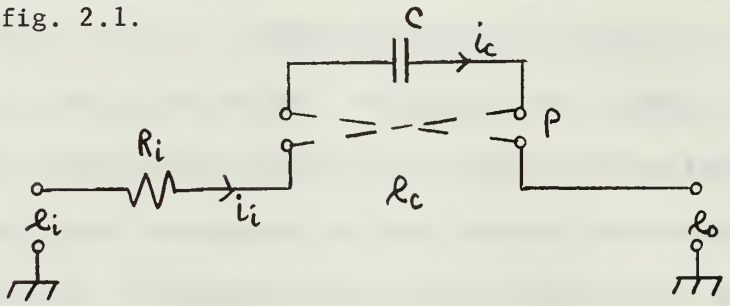

Figure 2.1 Commutated capacitor

The commutating function, P, is a unit square wave of the same frequency as the input signal, e_i. The following equations can be written for fig. 2.1:

$$e_c = \frac{1}{c}\int i_c \, dt \tag{2-1}$$

$$i_c = P \cdot i_i \tag{2-2}$$

$$e = P \cdot e_c \tag{2-3}$$

$$e = P \cdot \frac{1}{c}\int P \cdot i_i \, dt \tag{2-4}$$

$$e = \frac{1}{c}\int i_i \, dt \tag{2-5}$$

since $P \cdot P = 1$ both when P is in the low and in the high position.

Figure 2.2 shows how the capacitor is placed in the coupled RC commutated network.

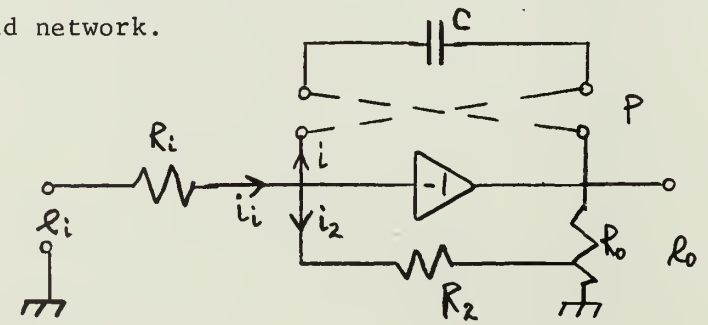

Figure 2.2 Coupled commutated network

Another variation of the commutated network is the uncoupled RC network shown in fig. 2.3.

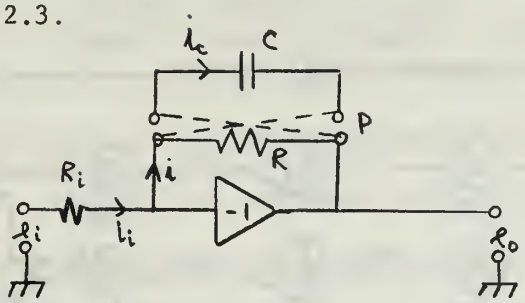

Figure 2.3 Uncoupled commutated network

Reference 1 proves that both variations of the commutated network can be represented by the circuit shown in fig. 2.4.

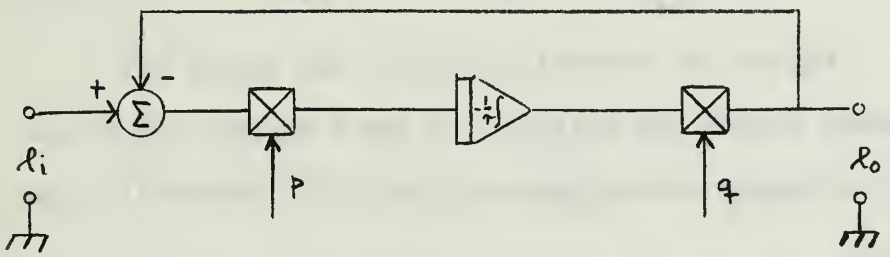

Figure 2.4 Equivalent circuit of commutated networks

The number of capacitors in the commutated network can be varied. For the following, four capacitors are used in the coupled version of the network. Figure 2.5 shows the circuit used in the analysis.

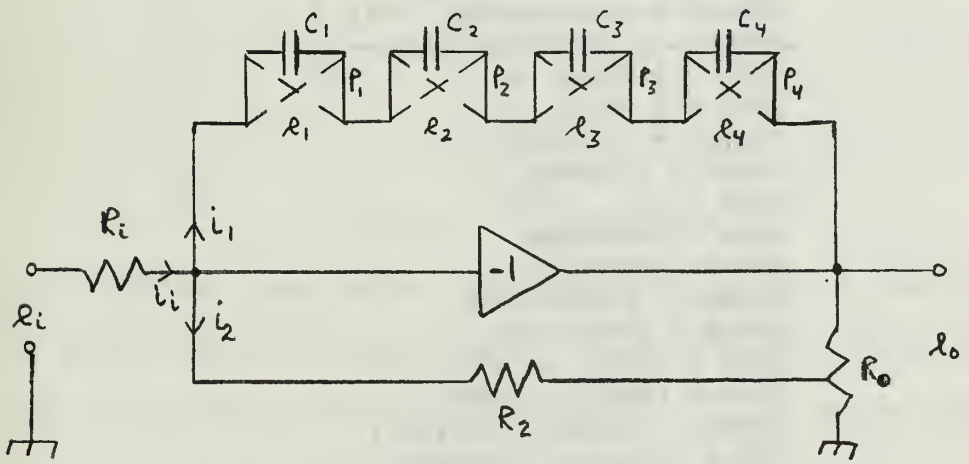

Figure 2.5 Four-capacitor commutated network

The equivalent network for the four-capacitor coupled commutated network is shown in fig. 2.6.

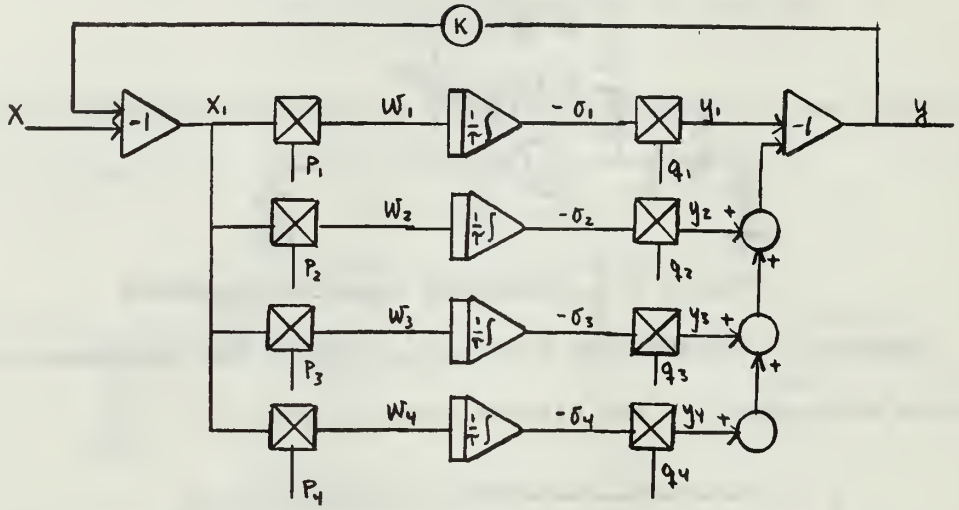

Figure 2.6 Equivalent circuit for figure 2.5

A computer program was written - in IBM's Digital Simulation Language - to simulate the network of fig. 2.5. Figure 2.7 shows the program used.

```
F = 1.
X = SIN(F*2.*3.1415*TIME)
ZONE = IMPULS (.0,1.00000)
ZTWO = IMPULS (.1250,1.00000)
ZTHREE = IMPULS (.2500,1.00000)
ZFOUR = IMPULS (.3750,1.00000)
FONE = PULSE(ZONE,.499)
FTWO = PULSE(ZTWO,.499)
FTHREE = PULSE(ZTHREE,.499)
FFOUR = PULSE(ZFOUR,.499)
PONE = 2.*FONE -1.
PTWO = 2.*FTWO -1.
PTHREE = 2.*FTHREE -1.
PFOUR = 2.*FFOUR -1.
XONE = -X - .95*Y
WONE = PONE*XONE
WTWO = PTWO*XONE
WTHREE = PTHREE*XONE
WFOUR = PFOUR*XONE
OONE = INTGRL(.0,WONE)
OTWO = INTGRL(.0,WTWO)
OTHREE = INTGRL(.0,WHTREE)
OFOUR = INTGRL(.0,WFOUR)
```

```
YONE = PONE*(-OONE)
YTWO = PTWO*(-OTWO)
YTHREE = PTHREE*(-OTHREE)
YFOUR = PFOUR*(-OFOUR)
Y = -( YONE + YTWO + YTHREE + YFOUR)
```

Figure 2.7 Computer program for simulation

The optimal value of the feed-back gain, K, was used. Reference 2 proves that the optimal value is 0.95 (1/(1+1/7 +1/9 +1/15 +1/17 + ...).

The modulating square wave, p, was generated in the following way: an impluse, Z_i, was generated at the beginning of every period. This impulse triggered a square-wave generator and the result, F_i, is shown in fig. 2.8.

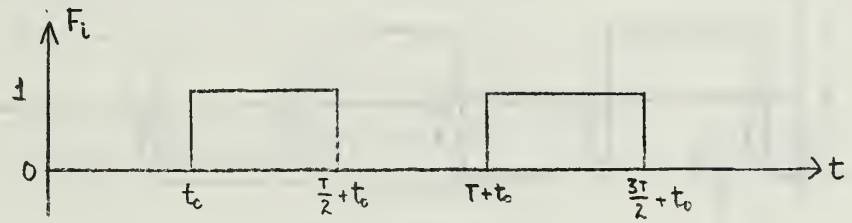

2.8

Figure 2.8 Square wave, F_i

The square wave, F_i, was multiplied by a factor of two and the DC-level was shifted minus one unit. The result is P_i as shown in fig. 2.9.

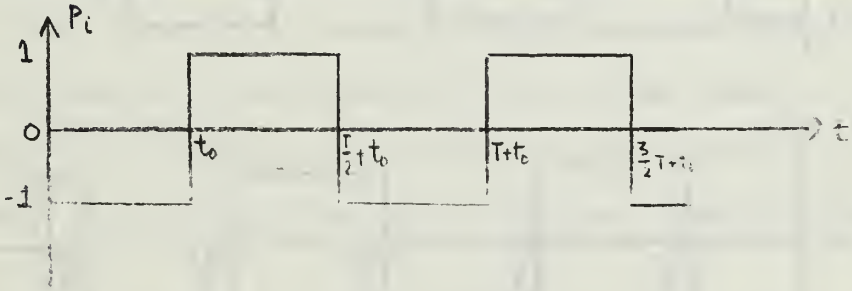

2.9

Figure 2.9 Square wave, P

The different square waves are delayed with respect to one another. P_2 is delayed T/8 with respect to P_1. P_3 is delayed T/8 with respect to P_2, and P_4 is delayed T/8 with respect to P_3. t_0 was chosen equal zero. Figure 2.10 shows the square waves as used in the program.

The following equations can be written for the commutating waveforms. P_1 is a unit square wave of period T, starting at t=0 thus f = 1/T Hz and $\omega_n = 2\pi/T$.

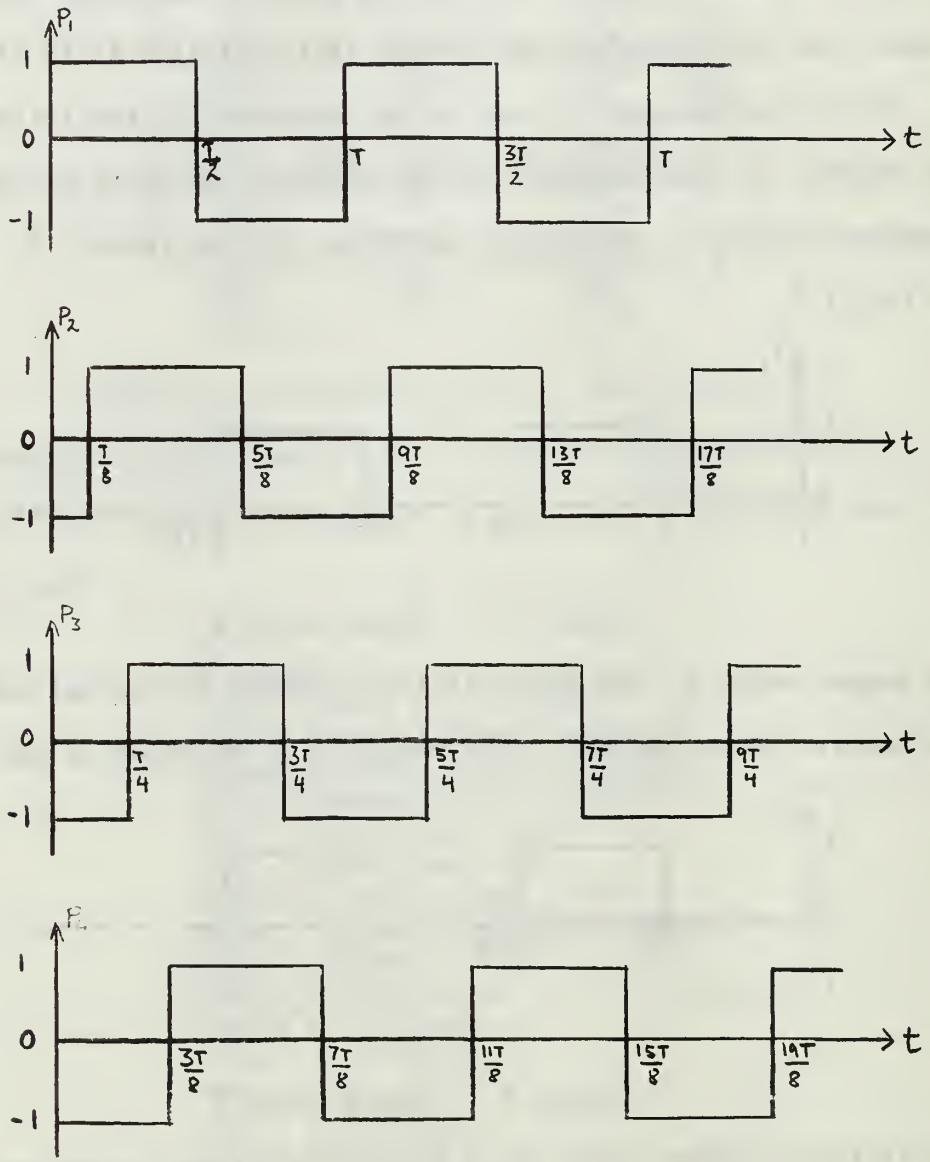

Figure 2.10 Commutating square waves

$$P_2 = P_1\left(\frac{2\pi}{T} - \frac{T}{8}\right) = P_1\left(\omega_n t - \frac{\pi}{4}\right) \tag{2-6}$$

$$P_3 = P_1\left(\frac{2\pi}{T} - \frac{T}{4}\right) = P_1\left(\omega_n t - \frac{\pi}{2}\right) \tag{2-7}$$

$$P_4 = P_1\left(\frac{2\pi}{T} - \frac{3T}{8}\right) = P_1\left(\omega_n t - \frac{3\pi}{4}\right) \tag{2-8}$$

The objective of the RC-commutated network is to construct a signal of same frequency but of opposite phase as the input signal. If this is the case the sum of the input signal and the output signal has zero component of the input frequency.

Figure 2.11 shows how this can be implemented.

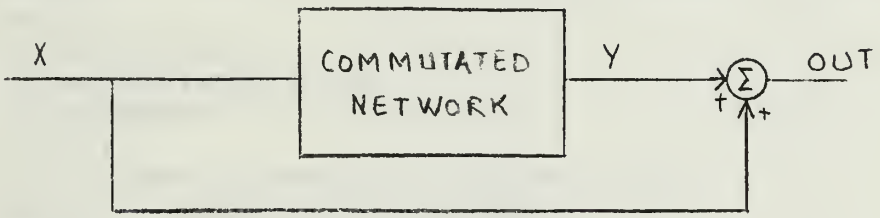

2.11

Figure 2.11 Filter configuration

Here OUT is the sum of X and Y. As a result of the square waves being applied to the capacitors, harmonics of the frequency of the input signal are present in the signal OUT. If N is the number of commutating capacitors in the network, ref. 2 shows that the following frequencies are present in the signals OUT and Y: $(2N-1)\omega_n$, $(2N+1)\omega_n$, $(4N-1)\omega_n$, $(4N+1)\omega_n$, etc.

In order to analyze the discontinous signal Y, a computer program was written. The object of the program was to calculate the components a_n and b_n in a series of the form

$$Y = \frac{a_0}{2} + \sum_{n=1}^{\infty}\left(a_n \cos n\omega_n t + b_n \sin n\omega_n t\right) \tag{2-9}$$

Figure 2.12 shows the program written in FORTRAN IV. Table I lists the component values a_n and b_n of the output signal Y.

It is seen from the table that the following components are dominant: 1st, 7th, 9th, 15th, 17th, 23rd, 25th, 31st, 33rd, 39th, 41st, 47th, 49th, etc. This is in agreement with theory given in ref. 2.

An investigation was made to find out if the value of t_0, the time where P_1 first goes to the value +1.0, had any effect on the output signal Y. The following phase delays were tried for the commutating wave-forms: $\pi/5$, $2\pi/5$, $3\pi/5$, and $4\pi/5$. The results showed that phase-delaying the commutating square waves does not change the output signal. The series of equation (2-9) still has the same coefficients.

```
FORTRAN
      SUBROUTINE TORIT(FNT,N,M,A,B)
      DIMENSION A(100),B(100),FNT(10500),C(100),PHI(100)
      WRITE(6,11)
   11 FORMAT(7X,'J',8X,'A(J)',  13X,'B(J)', 13X,'C(J)' , 13X, 'PHI(J)')
   60 AN=N
      COEF=2.0/(2.0*AN+1.0)
      CONST=3.141593*COEF
      S1=SIN(CONST)
      C1=COS(CONST)
      P = 1.0
      S=0.0
      J=1
      FNTZ=FNT(1)
   70 U2=0.0
      U1=0.0
      I=2*N+1
   75 UO=FNT(I)+2.0*P*U1-U2
      U2=U1
      U1=UO
      I= I-1
      IF(I-1) 80,80,75
   80 A(J)=COEF*(FNTZ+P*U1-U2)
      B(J)=COEF*S*U1
      K = J-1
      C(J) = SQRT((A(J))*(A(J)) + (B(J))* (B(J)))
      PHI(J) = -ATAN(B(J)/A(J))*57.2957795
      WRITE(6,12) K,A(J),B(J),C(J),PHI(J)
   12 FORMAT(3X,I5,1P4E17.7)
      IF(J-(M+1)) 90,100,100
   90 Q=C1*P-S1*S
      S=C1*S+S1*P
      P = Q
      J=J+1
      GO TO 70
  100 A(1)=A(1)*0.5
      RETURN
      END
```

Figure 2.12 Computer program for Fourier analysis

N	A	B
0	-4.0915914E-02	0.0
1	5.7432428E-02	-9.7068429E-01
2	-6.4395438E-04	-2.9122231E-03
3	6.7318883E-04	-3.3683525E-03
4	-8.5144676E-04	-6.8645878E-04
5	-1.0724834E-03	-1.2038115E-03
6	-1.3770524E-03	4.9475231E-05
7	1.2983000E-01	-5.7617463E-02
8	-1.4599903E-04	-4.4301525E-04
9	9.9531114E-02	-5.0481014E-02
10	1.1894142E-03	-1.2319605E-03
11	7.7437004E-04	-5.9847650E-04
12	2.1180733E-04	-9.1678812E-04
13	2.8510741E-04	-1.2260592E-04
14	-5.2539515E-04	-1.4881822E-03
15	4.4528384E-02	4.8904710E-02
16	3.3075595E-04	-3.5192422E-04
17	4.2879425E-02	4.1087449E-02
18	1.3891549E-03	5.6604668E-04
19	7.9694903E-04	3.0924985E-04
20	8.3581335E-04	-1.5659863E-04
21	1.0385311E-04	-2.5742664E-04
22	1.0932467E-04	-9.7328471E-04
23	-1.9760877E-02	3.8151786E-02
24	4.1980087E-04	1.3531574E-04
25	-1.6020168E-02	3.7231848E-02
26	-5.6435747E-05	1.4239037E-03
27	5.6750767E-05	8.6518889E-04
28	4.2703399E-04	7.1566226E-04
29	6.2502408E-04	8.1200222E-04
30	1.3039294E-03	6.7783101E-04
31	-3.1548135E-02	-3.6806425E-03
32	3.1624935E-05	4.2581698E-04
33	-3.0806191E-02	-1.3784338E-03
34	-1.3438673E-03	4.3319259E-04
35	-7.8415312E-04	3.8454239E-04
36	-5.2506500E-04	6.4045424E-04
37	-5.0879410E-04	8.5357740E-04
38	-1.7829986E-04	1.4619438E-03
39	-6.1985478E-03	-2.4380792E-02
40	-3.8792193E-04	1.8413758E-04
41	-7.8365095E-03	-2.3663379E-02
42	-8.8027469E-04	-1.1022575E-03
43	-6.6715851E-04	-5.9376331E-04
44	-7.9095364E-04	-2.7252291E-04
45	-9.7992225E-04	-1.5532831E-04
46	-1.4365583E-03	3.4710323E-04
47	1.6978830E-02	-1.1989255E-02
48	-3.2683252E-04	-2.9340992E-04
49	1.6212072E-02	-1.3255987E-02
50	7.0357858E-04	-1.2116958E-03

Table I Fourier coefficients of output signal Y

III. FREQUENCY RESPONSE OF FILTER

An investigation of the phase difference between output and input signals was done for frequencies within one decade on either side of the notch frequency, ω_n.

The frequency response was done for a notch frequency of one hertz and with a time constant of one second.

The equivalent network of fig. 2.6 was used for the frequency response study where the frequency of the input signal, x, was varied between 0.1Hz and 10.0 Hz.

A Fourier analysis was done of theoutput signal y. The program of figure 2.12 was used for the analysis. The phase difference between the input signal and the first harmonic of the output signal was calculated. The calculations were done for times when the phase of the input signal was zero. The phase, Φ_1, of the first harmonic of the output signal is

$$\Phi_1 = - \tan (B_1/A_1) \qquad (3\text{-}1)$$

Figure 3.1 shows the plot of phase versus frequency as obtained. The phase starts at zero degrees for low frequencies and goes to -90 degrees for frequencies slightly less than ω_n, jumps to +90 degrees for frequencies slightly above ω_n, and goes back to zero degrees for high frequencies.

The values obtained in the computer simulation are collected in Table II.

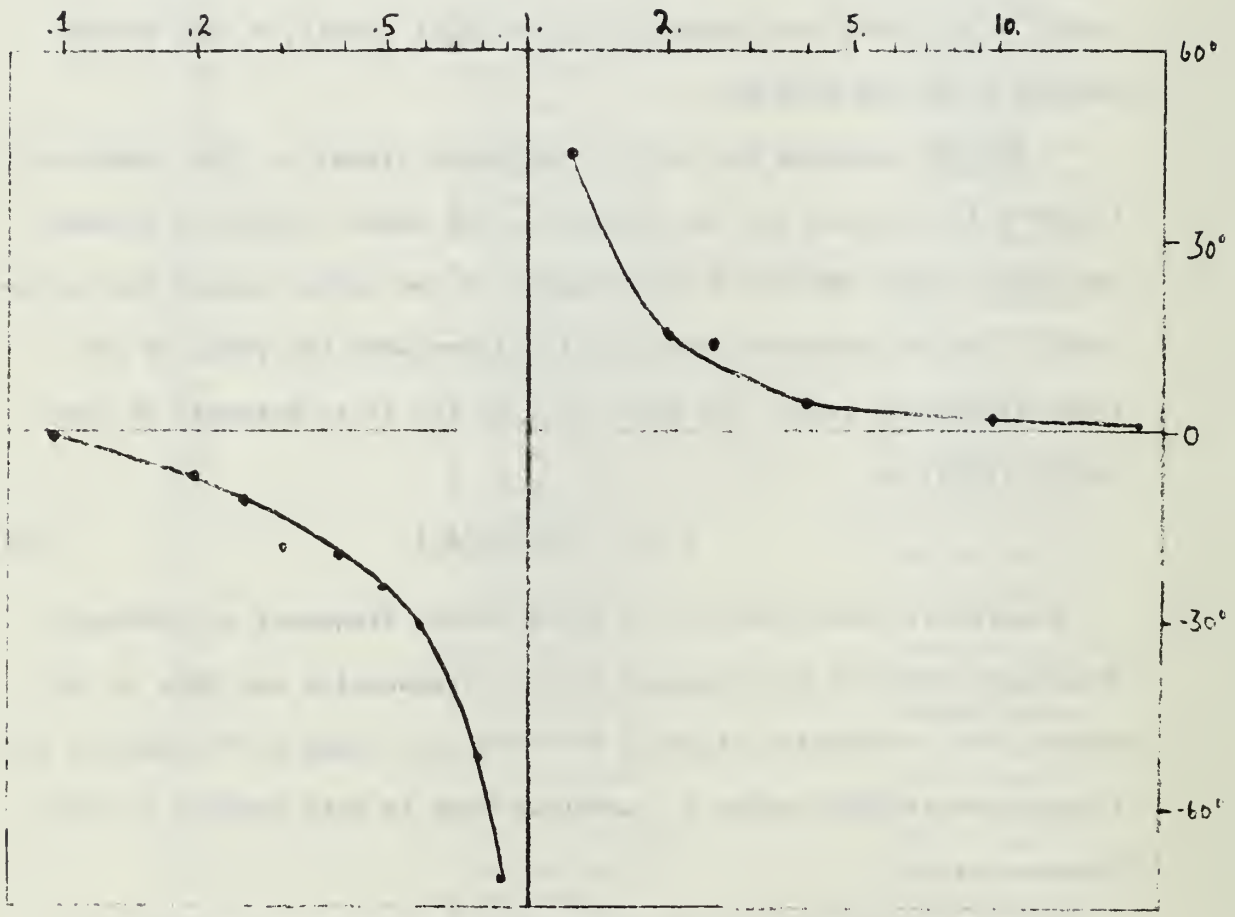

Figure 3.1 Frequency response of filter - phase

Frequency	Phase
0.1	- 1.51
0.2	- 7.40
0.25	-11.90
0.3	-18.59
0.4	-20.12
0.5	-24.00
0.6	-30.07
0.8	-51.54
0.9	-71.23
1.25	43.80
2.0	15.14
2.5	14.33
4.0	4.38
10.0	2.09
20.0	0.28

Table II Results of frequency response simulation - phase

IV. APPLICATIONS OF FILTER IN SERVOSYSTEMS

Computer simulations were done with the filter used in conjunction with servosystems. The objective of the filter was to suppress the component of frequency ω_n in the output signal C.

Example 1

A servosystem with the following transfer function was used in the first example:

$$\frac{c(s)}{x1(s)} = \frac{KMO/\omega_n^2}{s(0.00025\ s+1)\left(\frac{s^2}{\omega_n^2} + \frac{2\xi}{\omega_n}\ s+1\right)} \qquad (4\text{-}1)$$

Figure 4.1 shows the system that has the open-loop transfer function of equation (4-1).

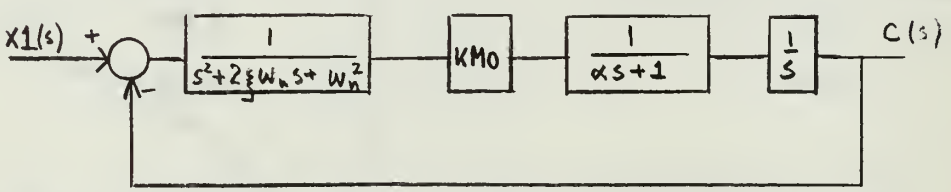

Figure 4.1 Servosystem of example 1

The following values were used: $\xi = 0.01$, $\omega_n = 2\pi f_i$ 2500 = 15708 rad/sec. Figure 4.2 shows how the filter was inserted in the servosystem. Figure 4.3 shows the Bode-plot for the system.

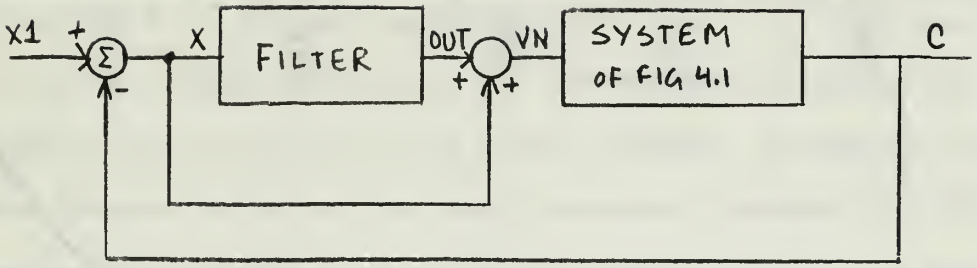

4.2

Figure 4.2 Compensated filter network

The signal VN is the sum of the signals OUT and VM. Since the fundamental component (frequency = ω_n) of the signal OUT is 180 degrees out of phase with the signal VM, the sum signal VN will have no component of frequency ω_n. The computer simulation of the system of fig. 4.1 was carried for different values of the gain KMO. Figures 4.4 - 4.6 show the time responses of the system to a unit step input for different values of KMO. It is seen that the output of the system when the filter is inserted is much smoother than the output of the system without the filter inserted, and it does not contain any component of frequency ω_n.

It is also seen that as the gain KMO is increased, the oscillations of the filtered output also increase in magnitude, but their amplitudes in the filtered output are still much smaller than their amplitudes in the unfiltered output signal. While the unfiltered output signal becomes unstable, the filtered output is still stable. An analysis of the output signal C shows that the dominant frequency of the signal varies as a function of the gain KMO. The dominant frequency is found to be the frequency where the magnitude curve of the Bode-plot crosses the zero-decibel axis.

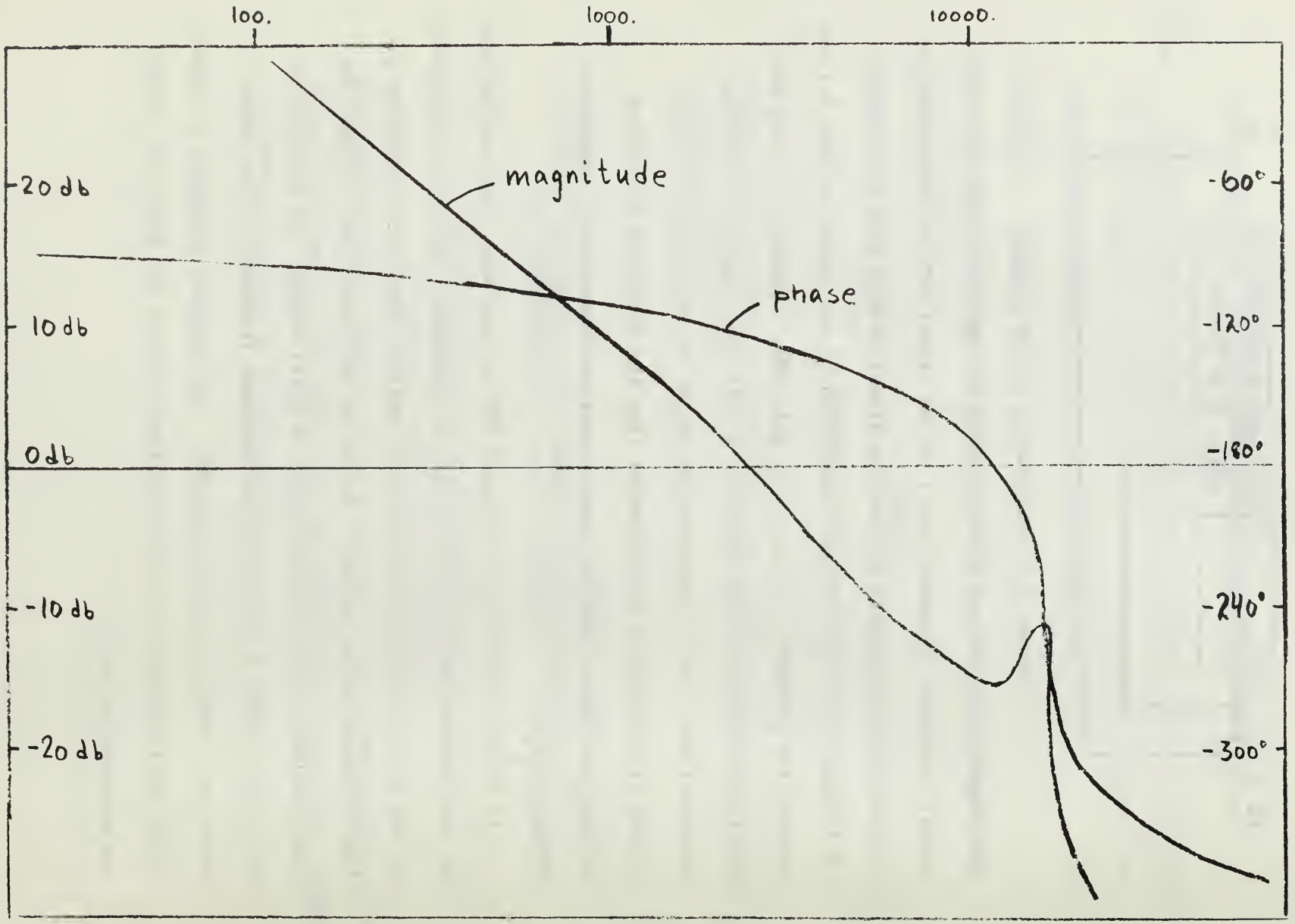

Figure 4.3 Bode plot of system of figure 4.1

Example 2 - 4

In examples 2 - 4 the same servosystem was used. Only the value of the gain KMO was changed. Figures 4.7 - 4.9 show the Bode-plots for the servosystem with and without the filter inserted. In example 2 the notch frequency is set at the phase cross-over (frequency $\doteq$ 15708 rad/sec). In example 3 the notch frequency of the filter is set at the magnitude cross-over of the Bode-plot. Finally in example 4 the notch frequency is set one decade below magnitude cross-over (frequency $\doteq$ 314 rad/sec).

The computer simulations for the time responses for examples 2 - 4 agreed with the expected results.

In example 2 the unfiltered output is stable with a phase margin of about 13 degrees. The output when the filtered is in the network has less phase margin but is still stable.

In example 3 the unfiltered output is stable with a phase margin of about 18 degrees. As seen from the Bode-plot for the system with the filter in the circuit the output is now unstable.

In example 4 the unfiltered output is identical to that of example 3. The notch frequency, however, is now one decade below the frequency ω_n, and the filter's frequency responses are now back to 0db and 0 degrees for magnitude and phase plots respectively at the gain cross-over. The filter has thus no influence on the output signal.

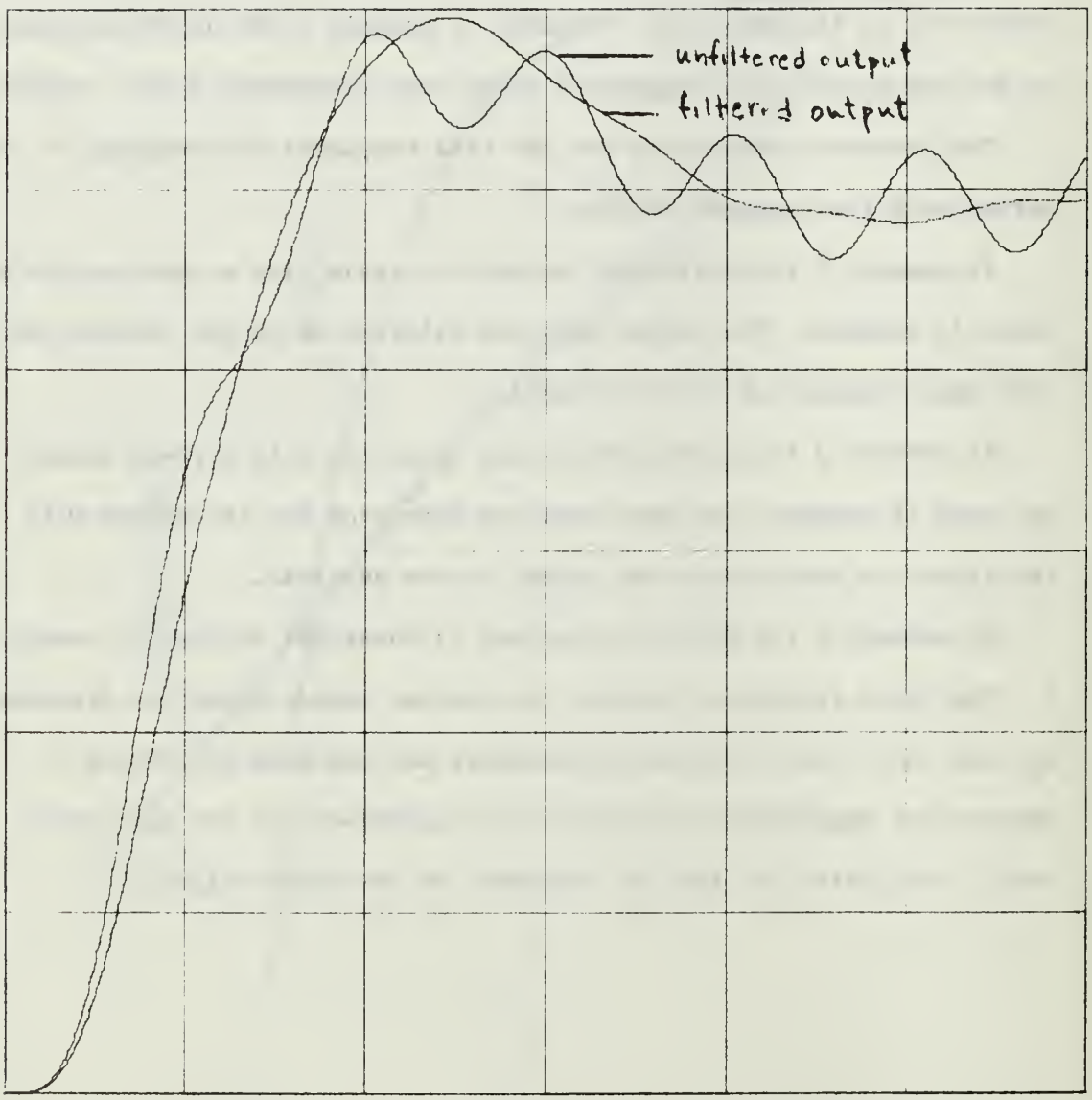

Figure 4.4 Time response to unit step input. $KM0=8.636 \times 10^{11}$

Scale: X=0.0004 sec/in, Y=0.2 units/in.

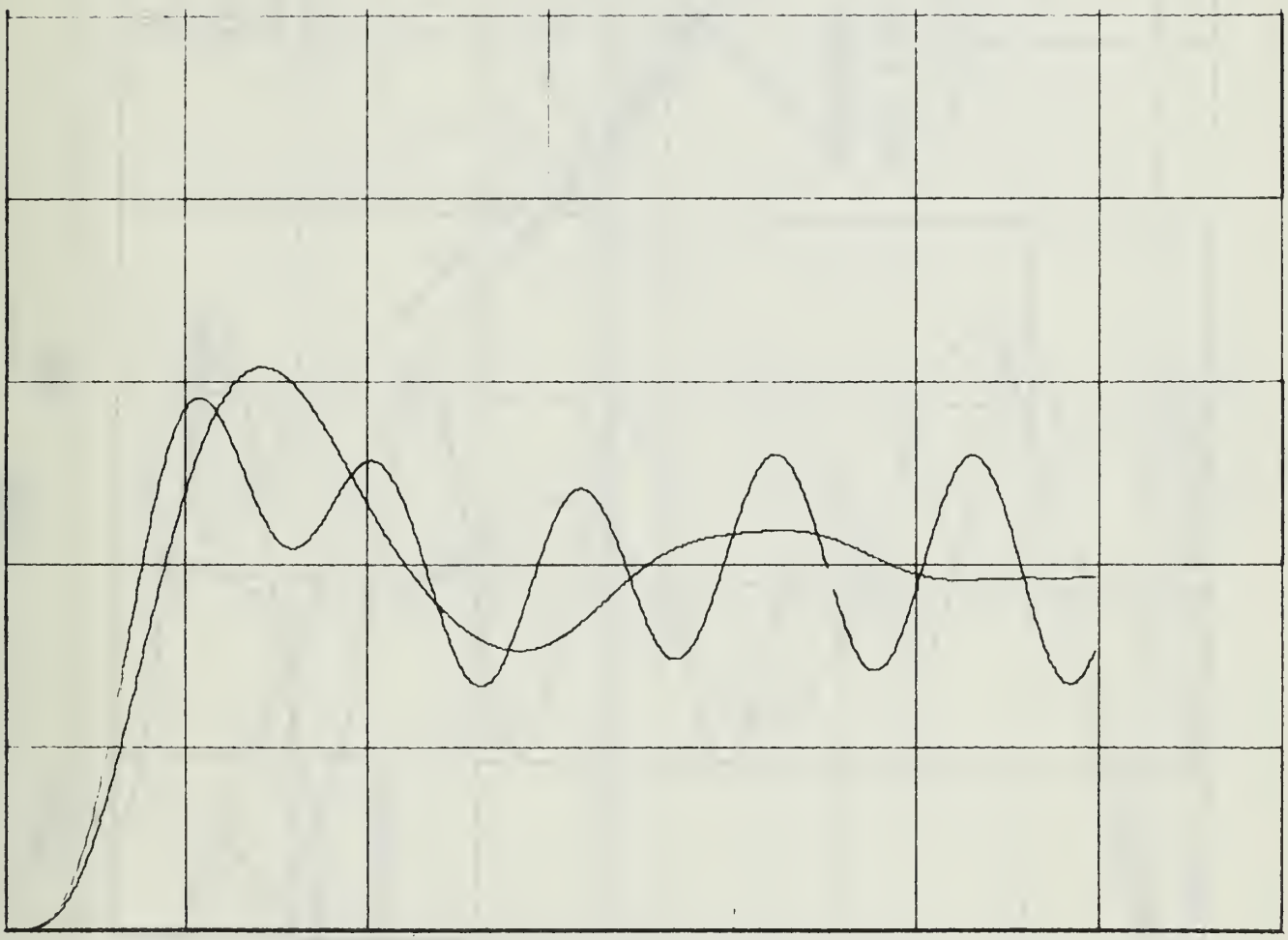

Figure 4.5 Time response to unit step input.KMO=2.0×10^{12}

Scale: X=0.0004 sec/in, Y=0.2 units/in.

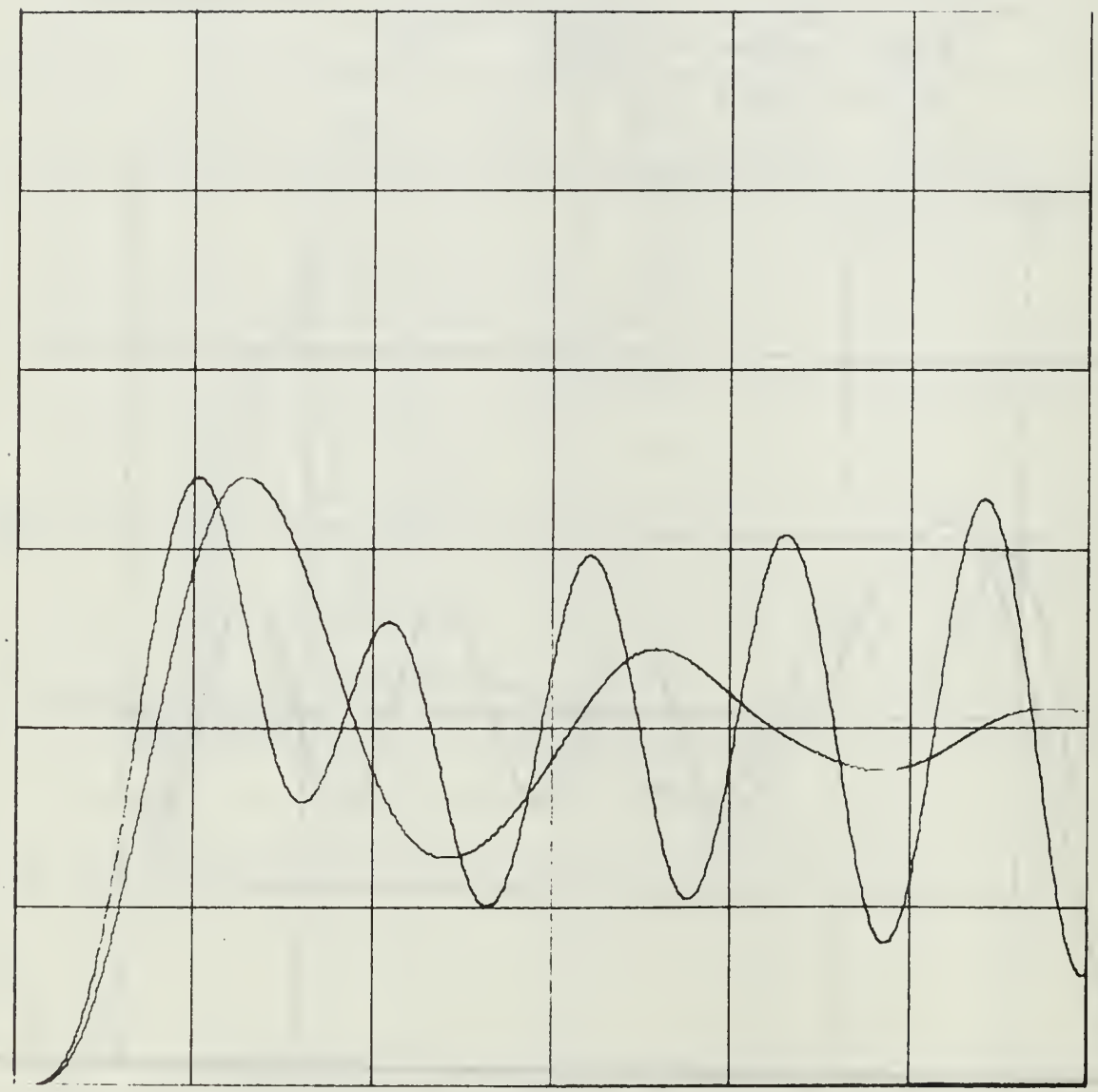

Figure 4.6 Time response to unit step input.KMO=2.5×10^{12}

Scale: X=0.0004 sec/in, Y=0.2 units/in.

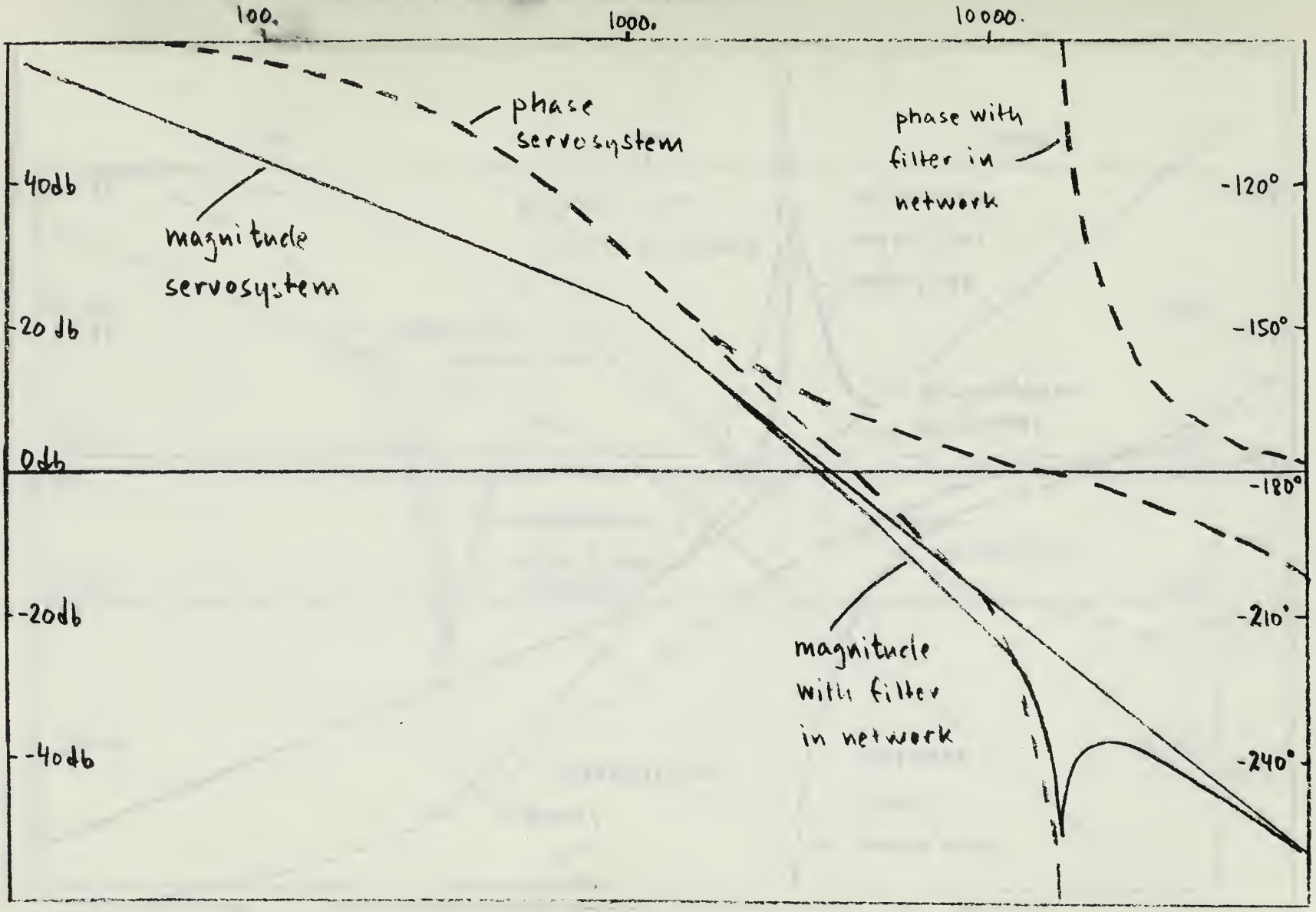

Figure 4.7 Bode-plot for example 2

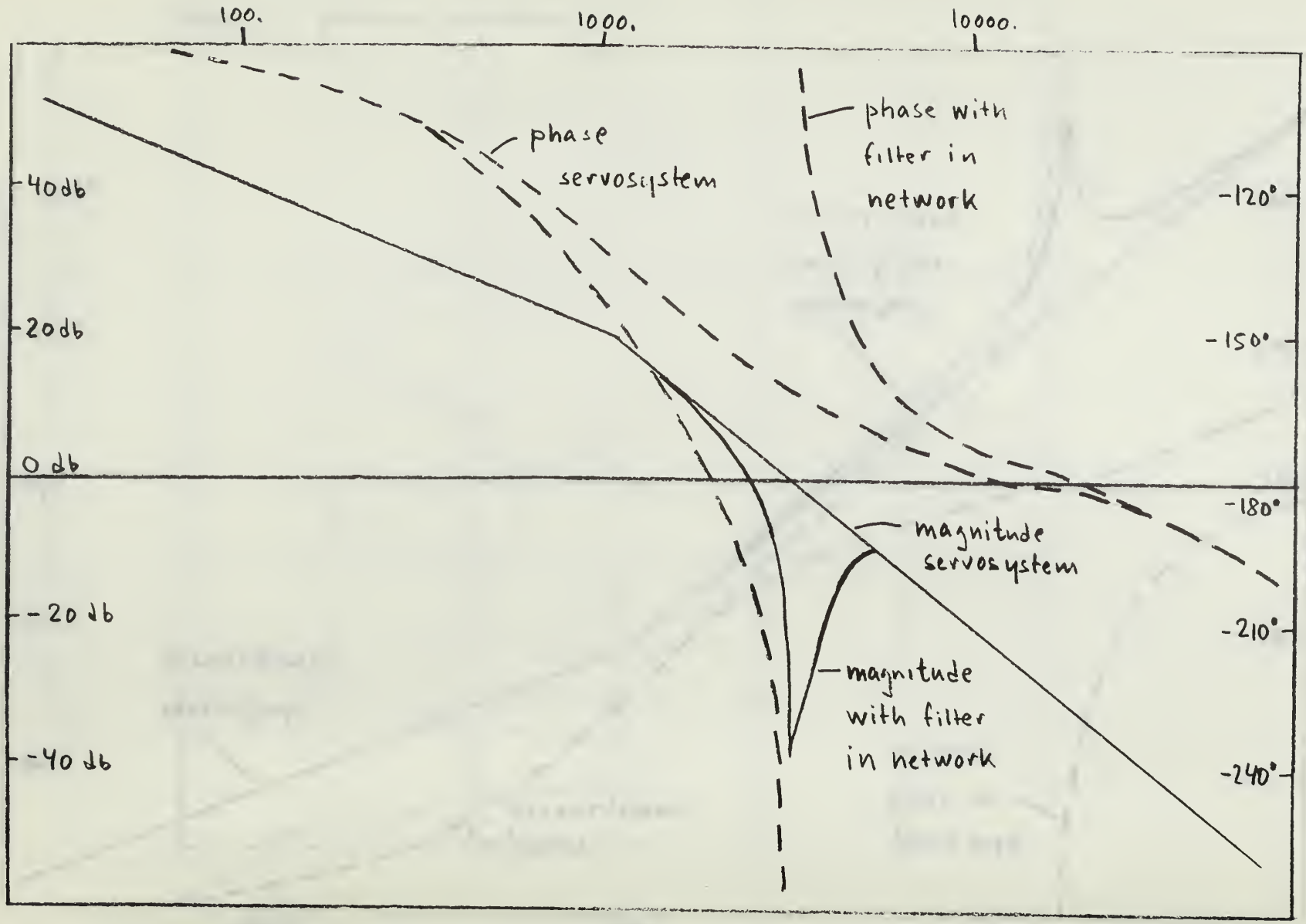

Figure 4.8 Bode-plot for example 3

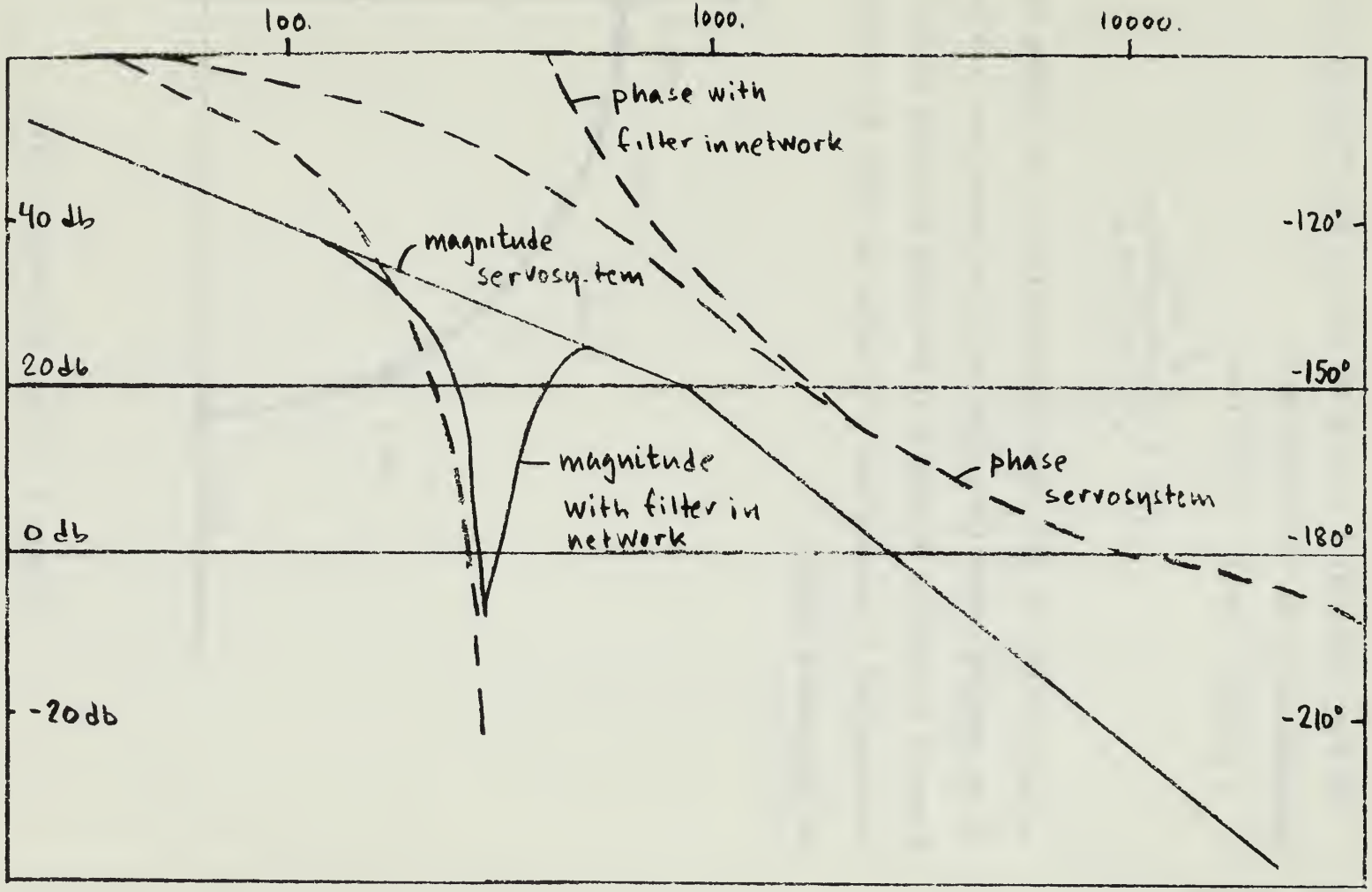

Figure 4.9 Bode-plot for example 4

V. APPROXIMATION OF FILTER TRANSFER FUNCTION

As seen from fig. 3.1 the phase part of the frequency response is discontinous at the notch-frequency.

A transfer function of the form

$$T(s) = \frac{s^2 + \omega_n^2}{s^2 + 2\xi\,\omega_n s + \omega_n^2} \qquad (5\text{-}1)$$

is seen to have the same phase characteristic. By varying the value of the damping factor the curvature of the phase curve can be changed. Figure 5.1 shows the locations of the poles and zeros of the transfer function T(s) in the s-plane. The poles are shown for different values of the damping factor.

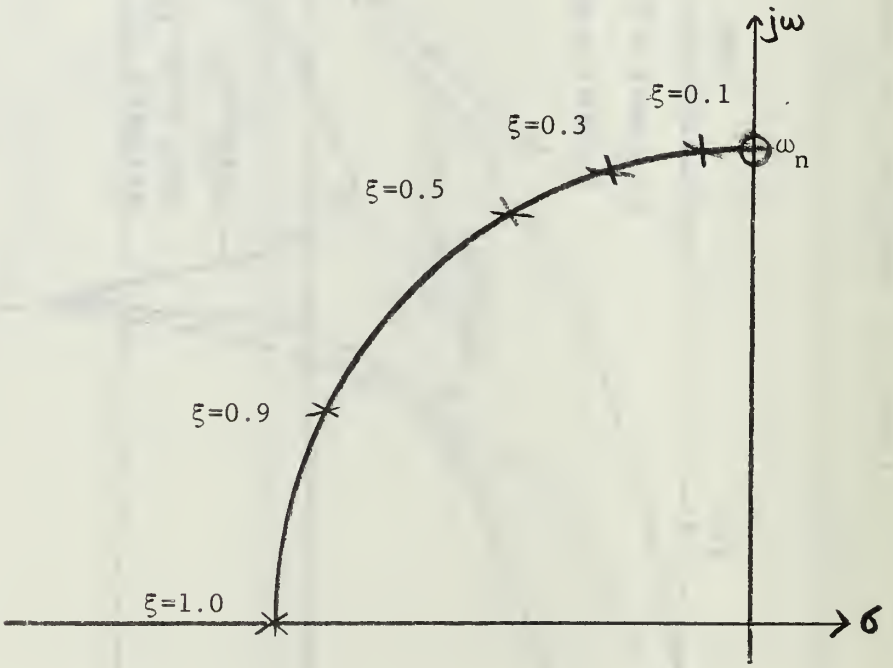

Figure 5.1 Poles and zeros of T(s)

Figure 5.2 shows the Bode-plot of T(s) and of the commutating network filter as obtained in chapter III.

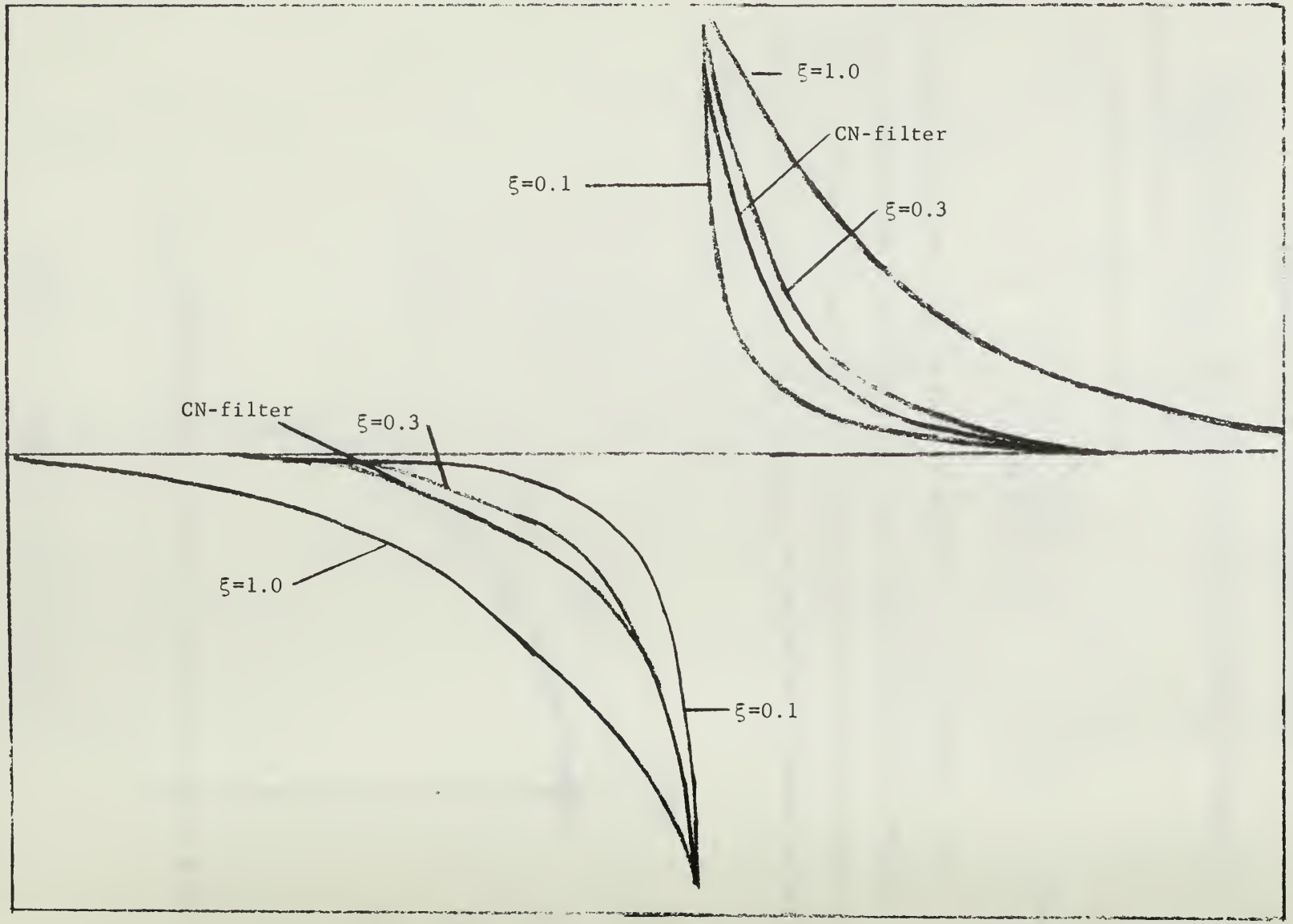

Figure 5.2 Bode-plot of T(s) - phase

VI. CONCLUSION

The commutated network filter has a highly selective bandpass filter characteristic where the center frequency of the bandpass frequency-response curve can be easily varied by changing the frequency of the commutating functions.

The filter can be approximated by a linear second-order transfer function for design purposes. The transfer function has two zeros on or very close to the imaginary axis and two poles on a circle with radius ω_n. The location of the poles can be changed depending on the value of the damping factor.

APPENDIX A

TIME RESPONSES OF SERVOSYSTEM

A compensated servosystem with open-loop transfer function

$$\frac{c(s)}{xi(s)} = \frac{KMO}{(\alpha s+1)\ (s^2+2\xi\ \omega_n s+\omega_n^2)} \qquad \text{(A-1)}$$

was used in example 1, chapter IV to get time responses to a unit step input for the system with and without the filter inserted.

Additional simulations were carried out for different combinations of the natural frequency ω_n and the damping factor ξ. Figure A.1 shows which combinations of ω_n and ξ were used.

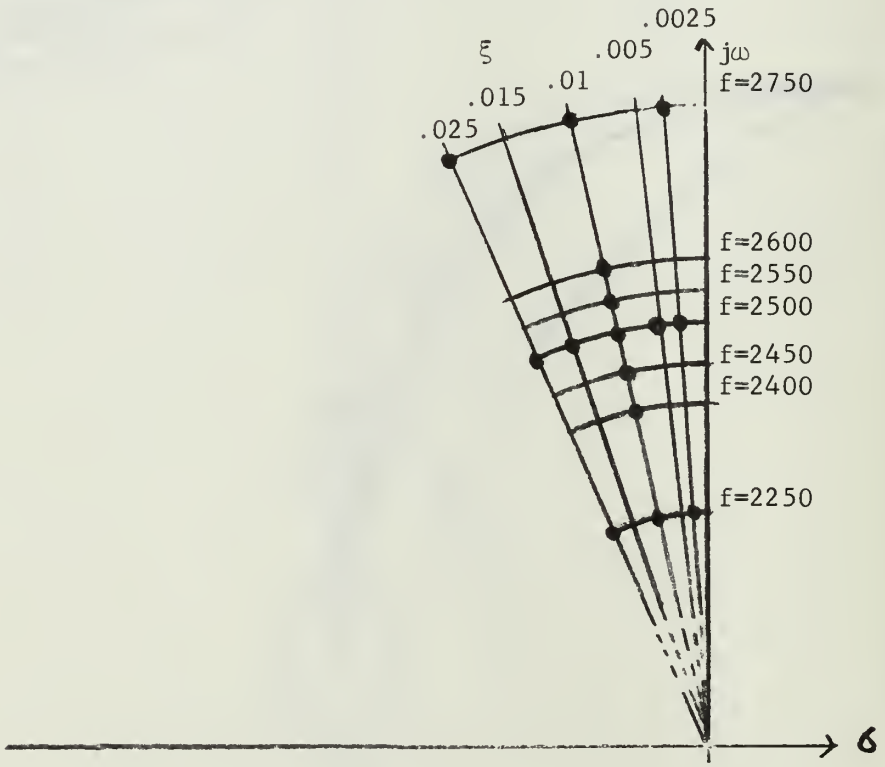

Figure A.1 Values used for time responses

Table III lists the values used for KMO, ω and ξ.

Figure	$\omega_n/2\pi$	ξ	KMO/10^{11}	X-scale sec/in	Y-scale units/in
A.2	2450	0.010	8.813	0.0004	0.2
A.3	2550	0.01	8.463	0.0004	0.2
A.4	2500	0.005	8.636	0.0004	0.2
A.5	2500	0.015	8.636	0.0004	0.2
A.6	2400	0.01	8.986	0.0004	0.2
A.7	2600	0.01	8.290	0.0004	0.2
A.8	2500	0.0025	8.636	0.0004	0.2
A.9	2500	0.020	25.000	0.0004	0.5
A.10	2500	0.020	8.636	0.0004	0.2
A.11	2250	0.010	9.499	0.0004	0.2
A.12	2250	0.0025	9.499	0.0004	0.2
A.13	2250	0.020	9.499	0.0004	0.2
A.14	2750	0.01	7.772	0.0004	0.2
A.15	2750	0.0025	7.772	0.0004	0.2
A.16	2750	0.02	7.772	0.0004	0.2

Table III Values used for computer-simulation

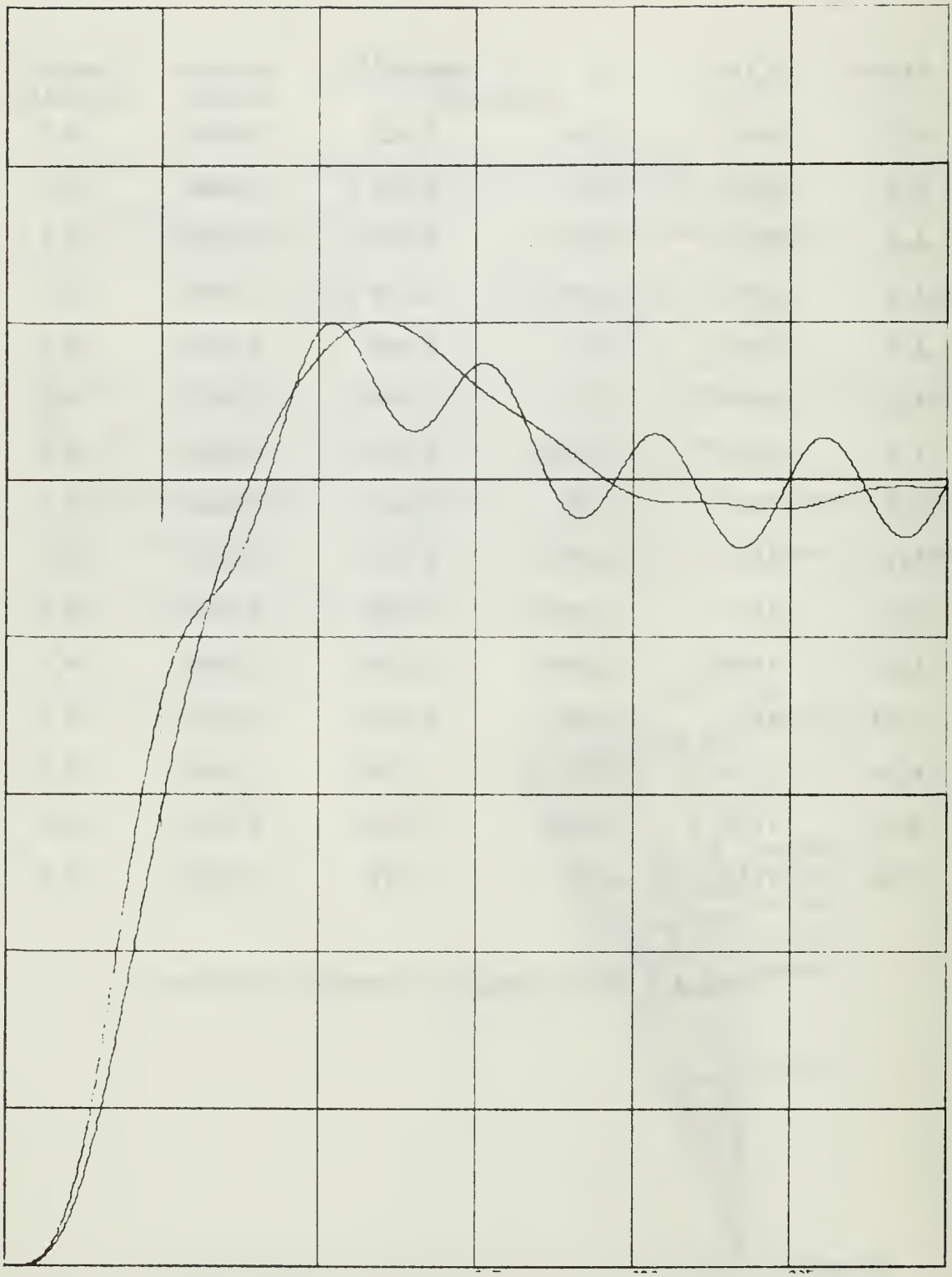

Figure A.2 Time response to unit step input

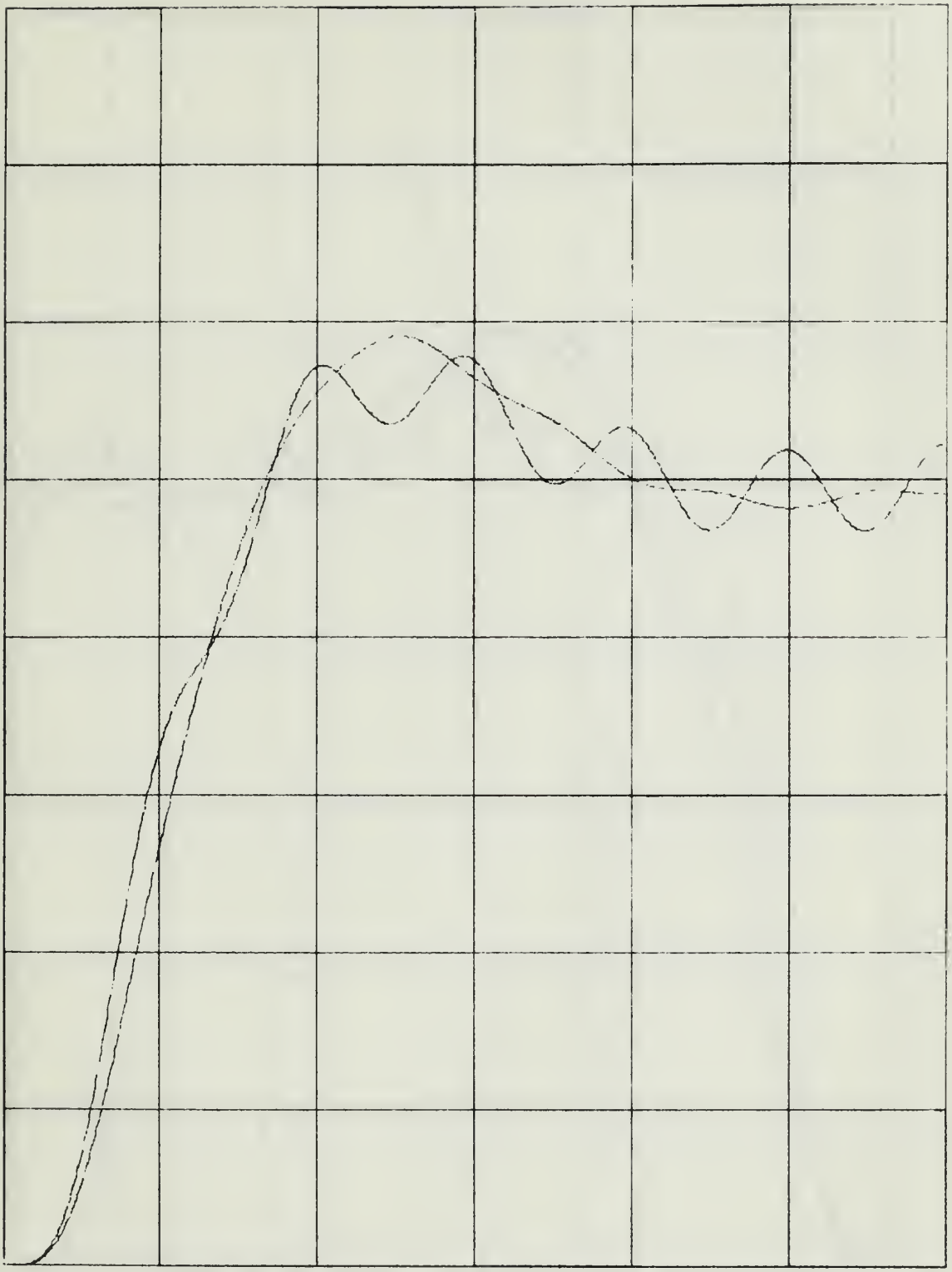

Figure A.3 Time response to unit step input

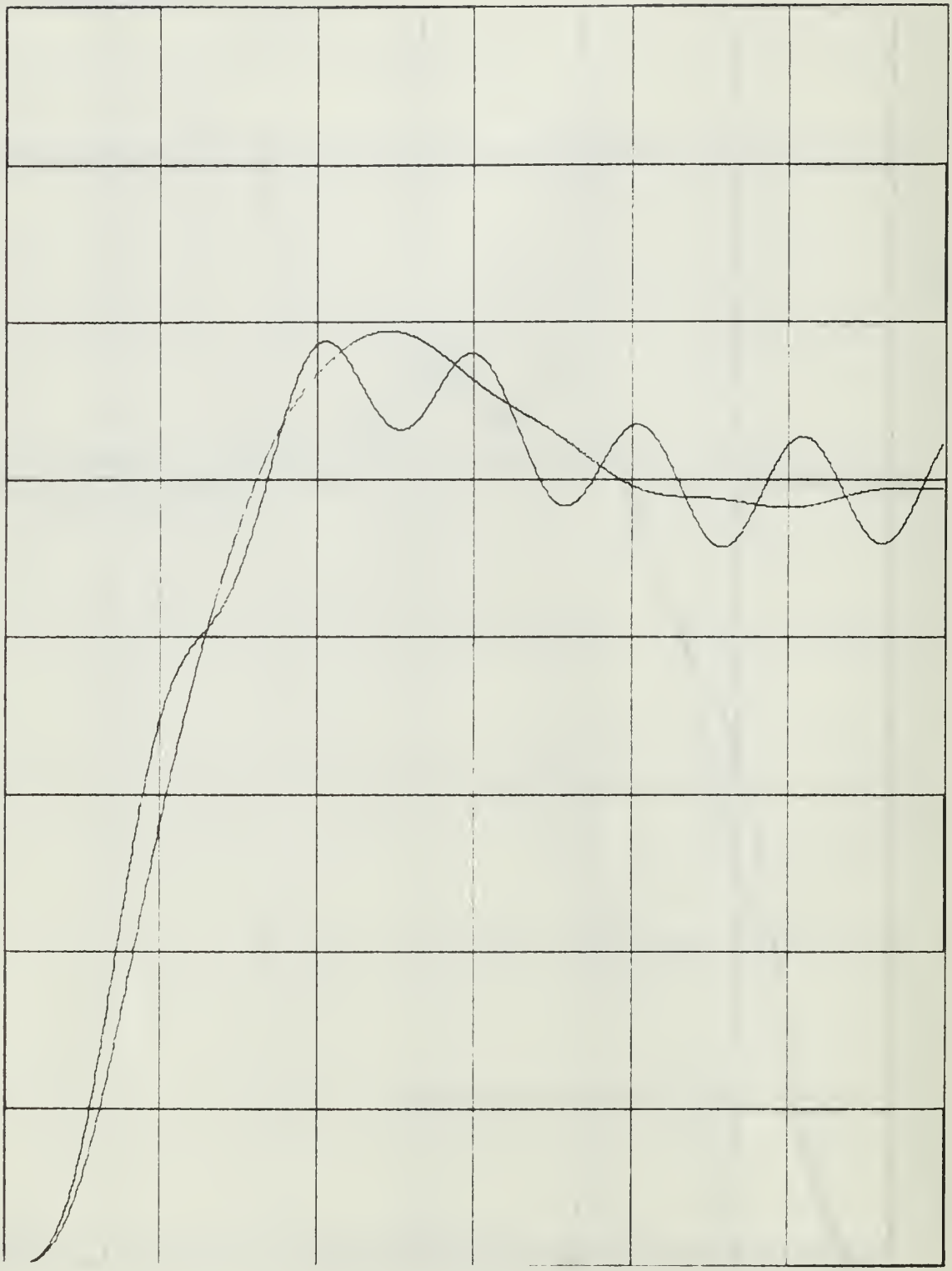

Figure A.4 Time response to unit step input

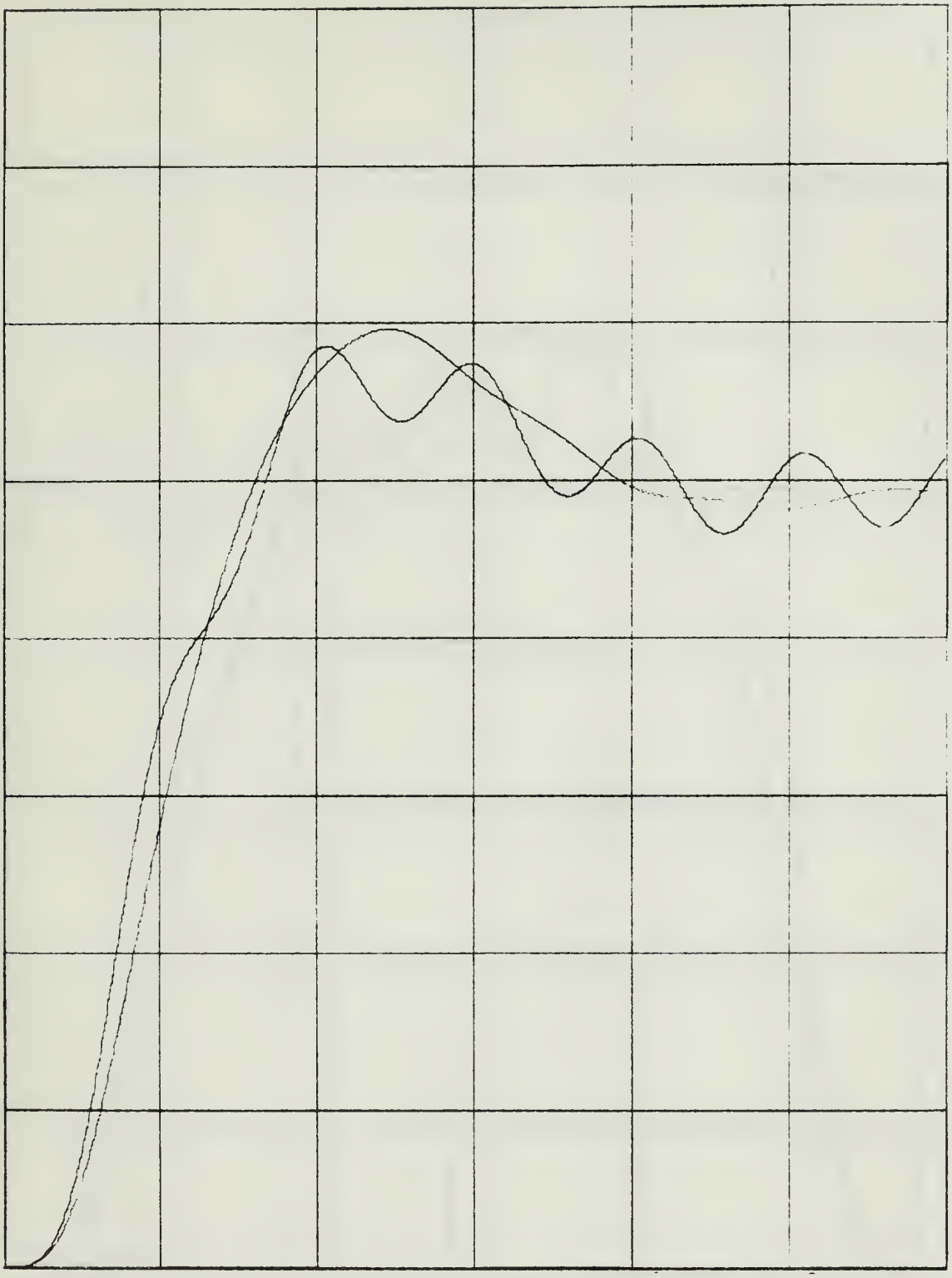

Figure A.5 Time response to unit step input

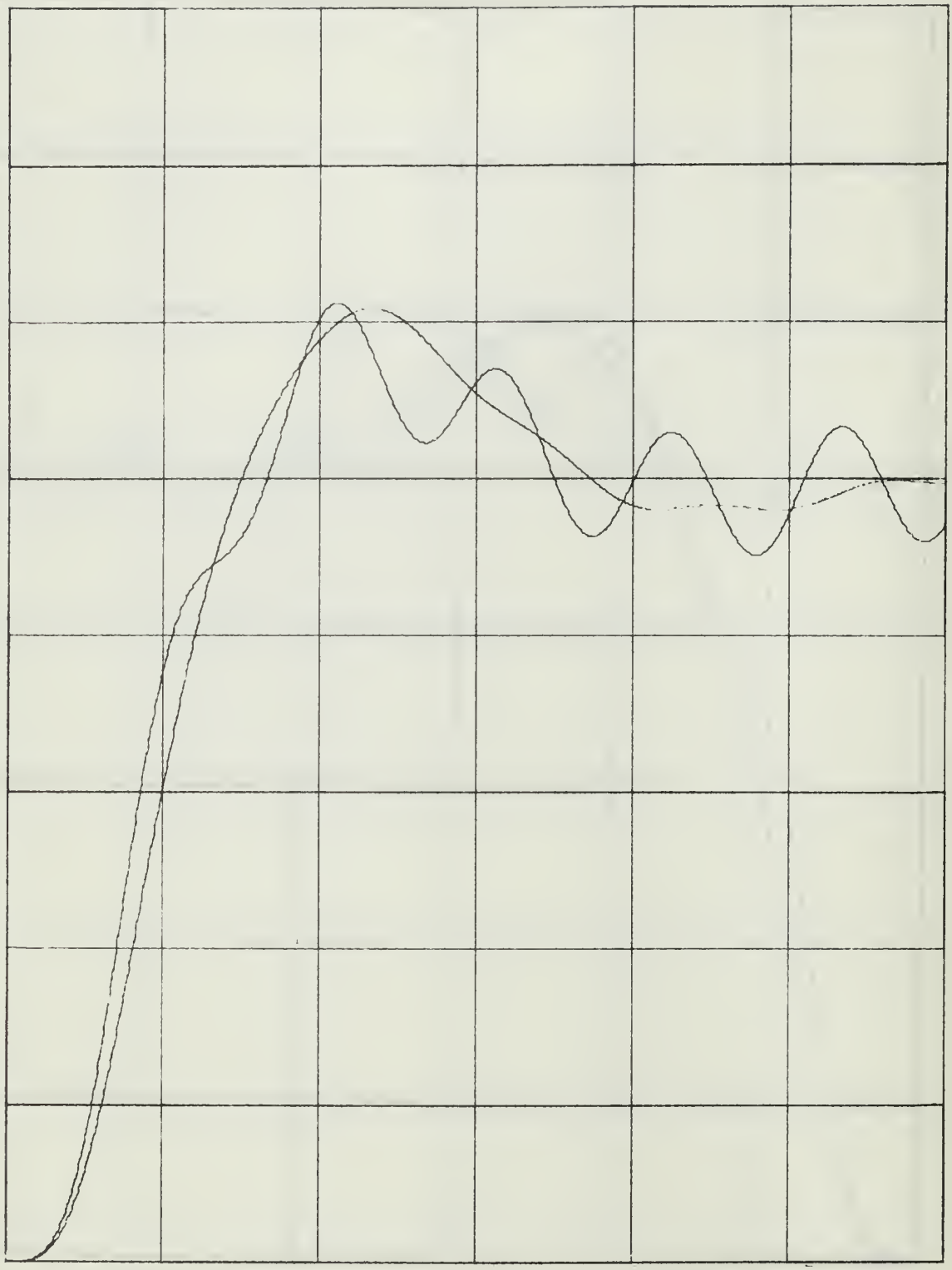

Figure A.6 Time response to unit step input

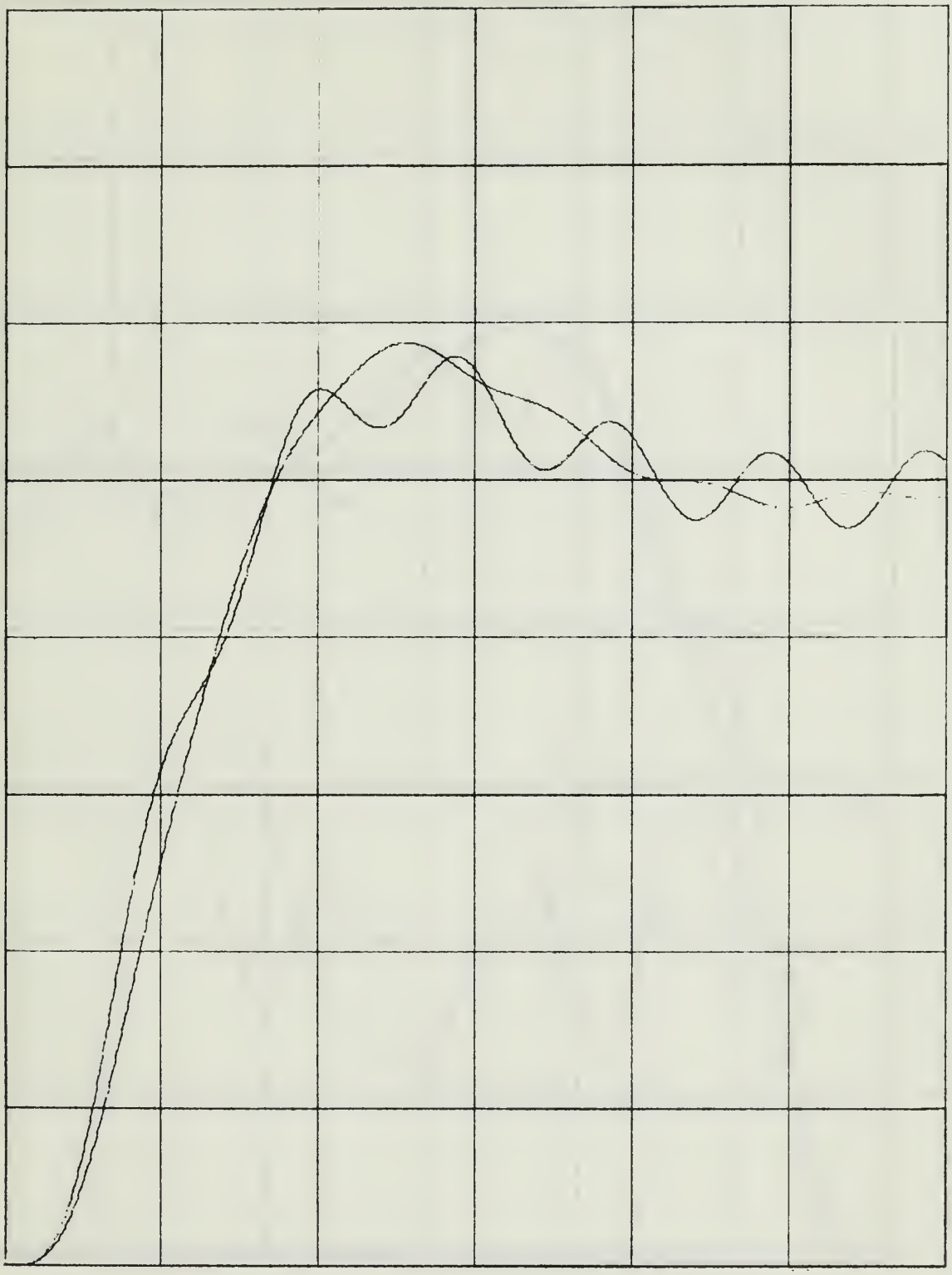

Figure A.7 Time response to unit step input

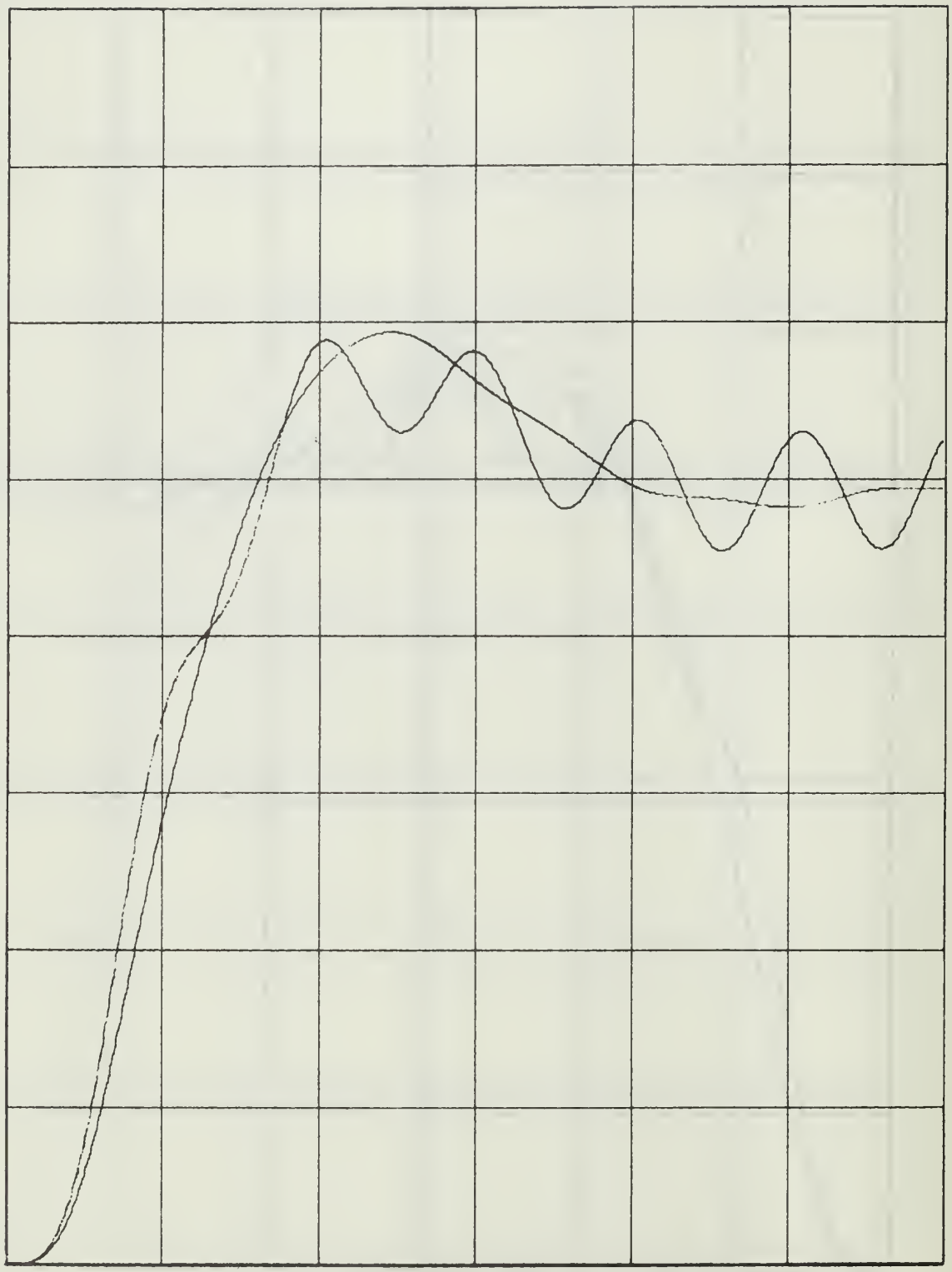

Figure A.8 Time response to unit step input

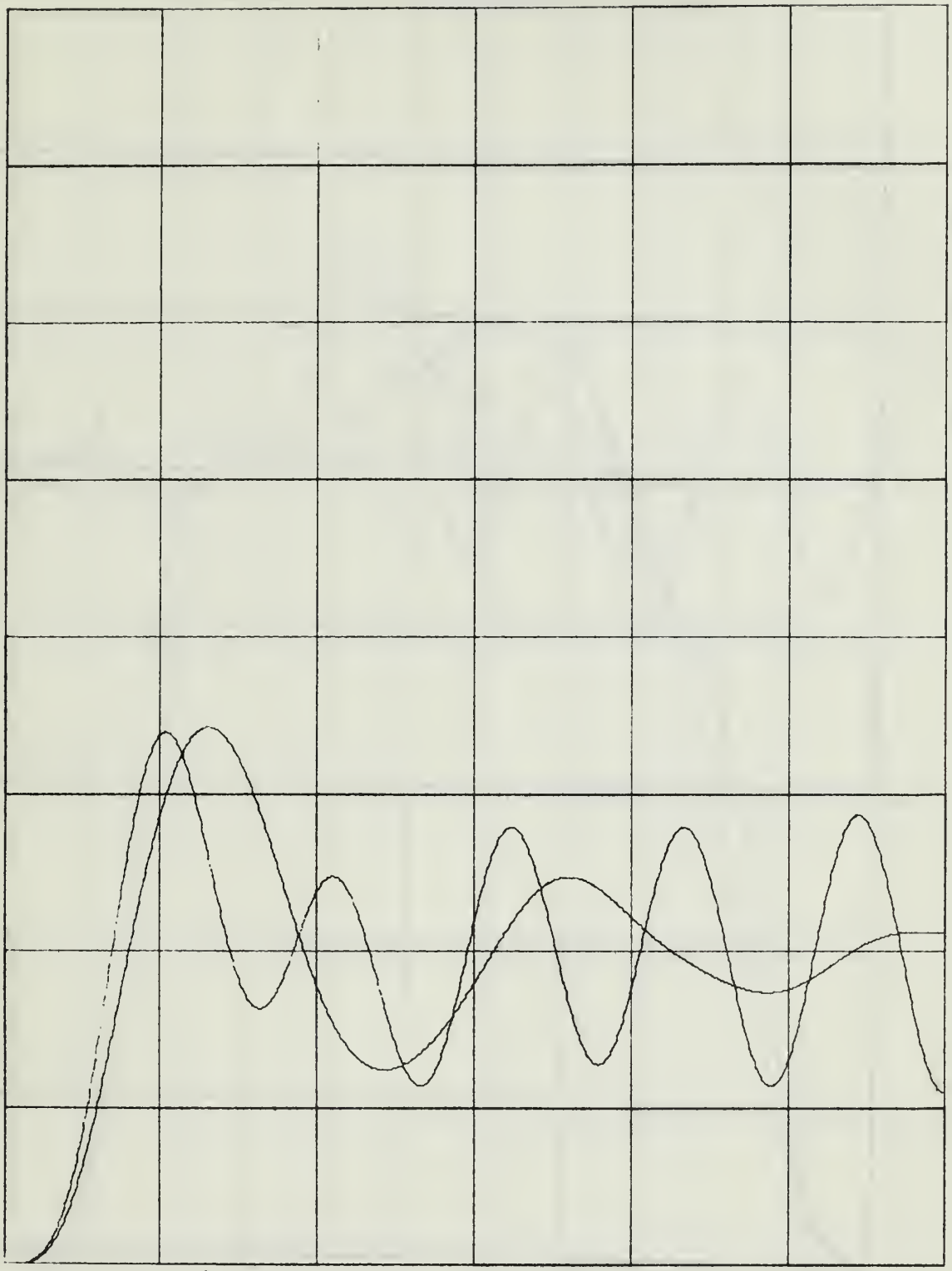

Figure A.9 Time response to unit step input

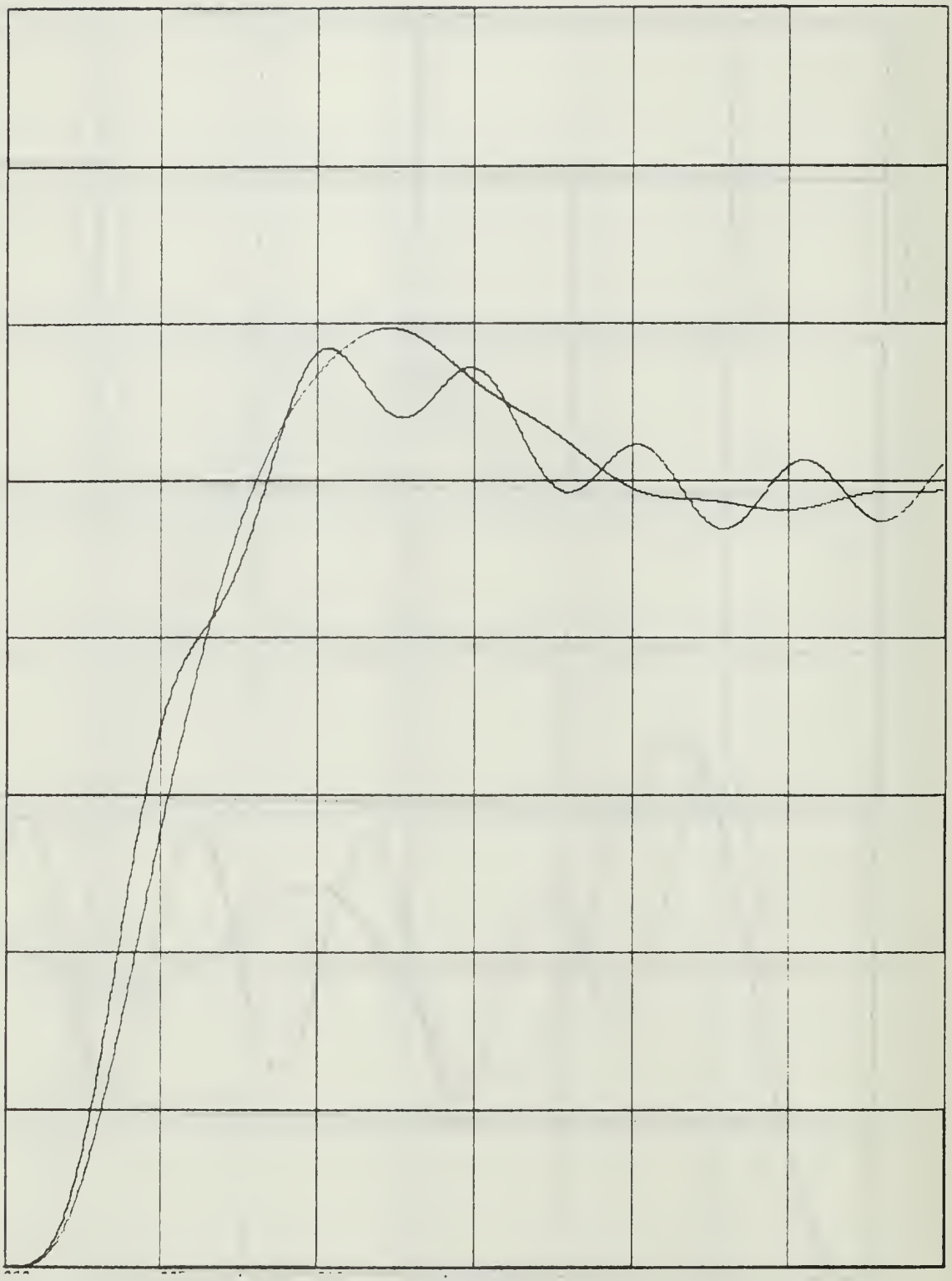

Figure A.10 Time response to unit step input

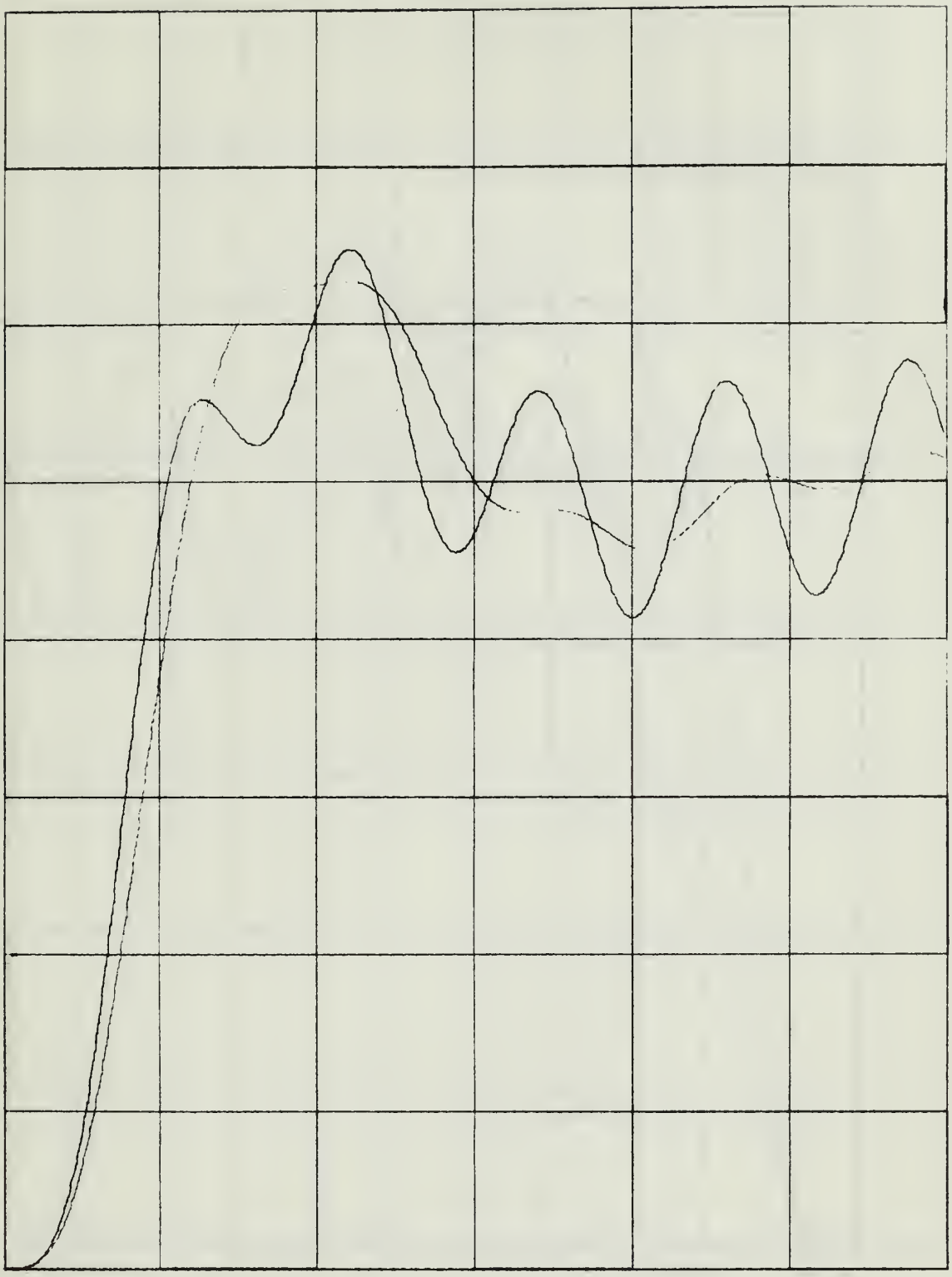

Figure A.11 Time response to unit step input

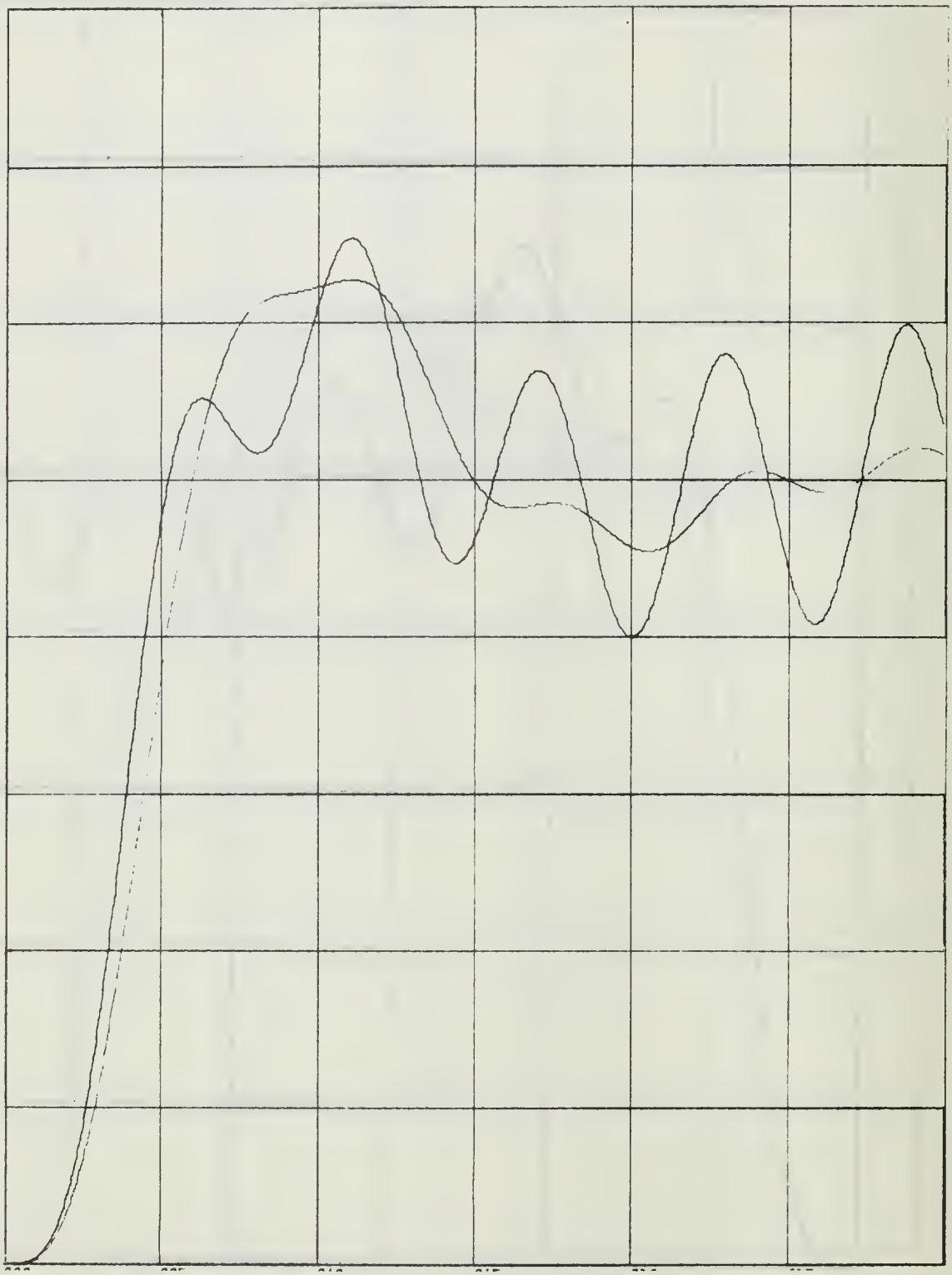

Figure A.12 Time response to unit step input

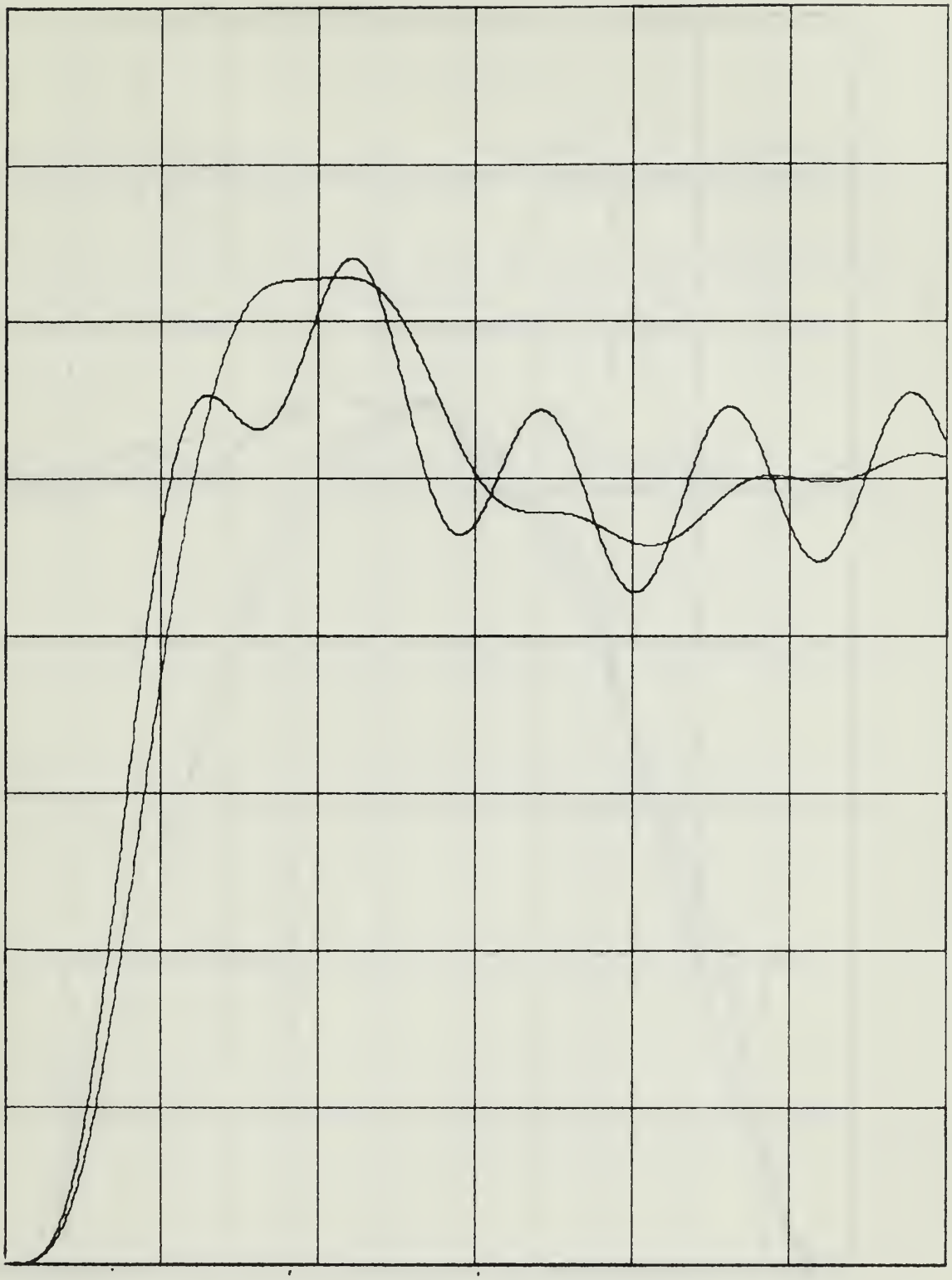

Figure A.13 Time response to unit step input

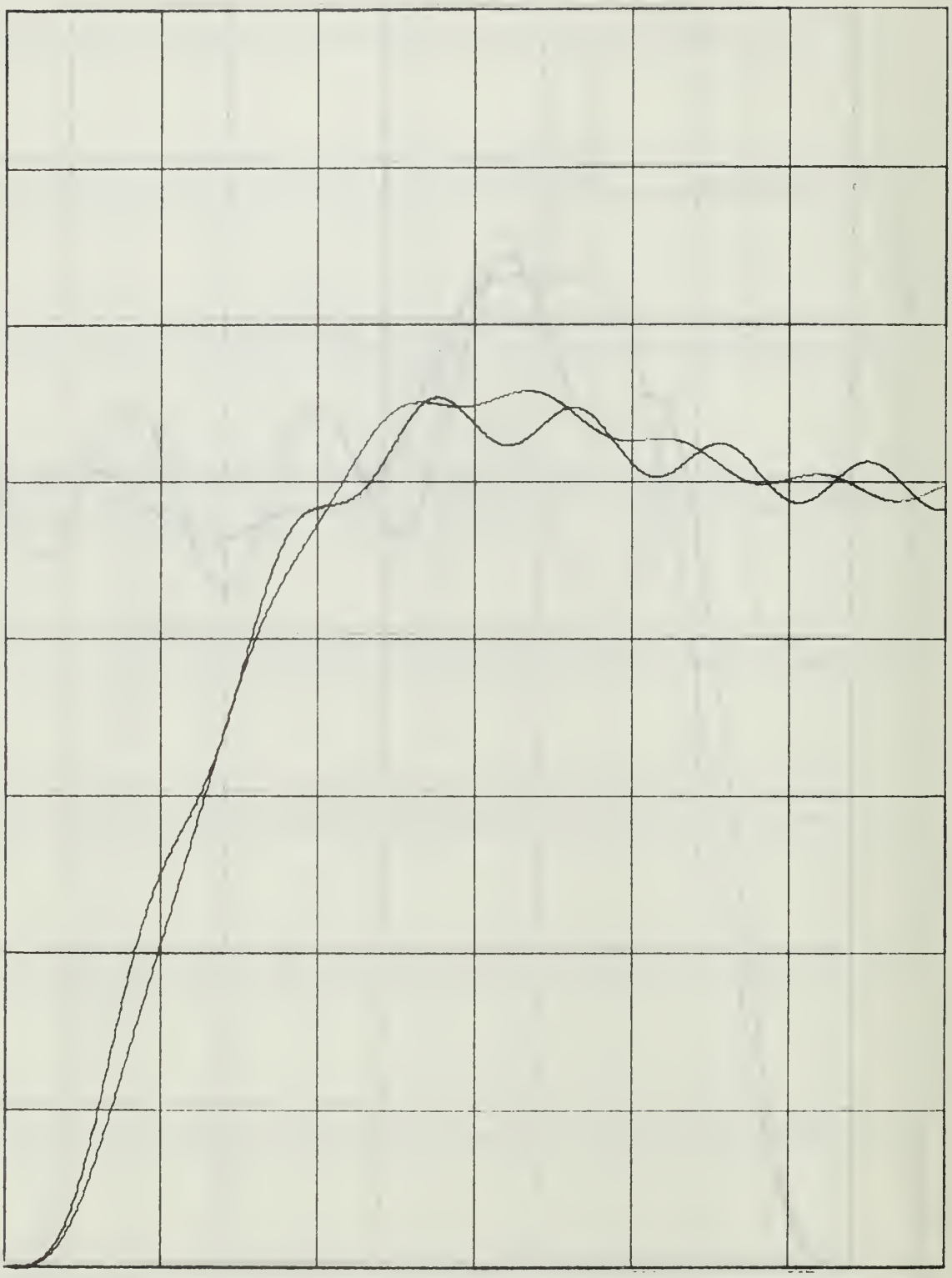

Figure A.14 Time response to unit step input

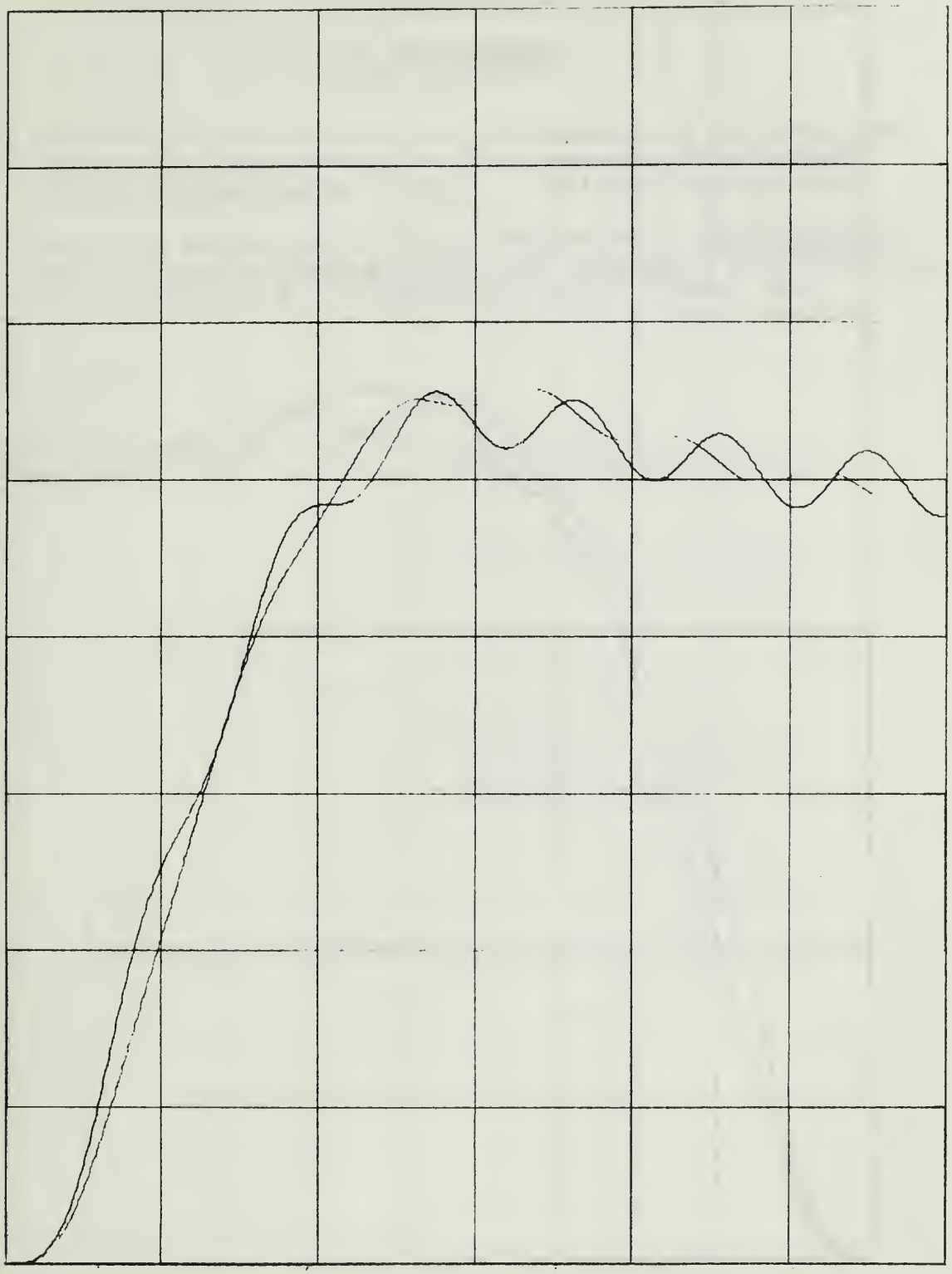

Figure A.15 Time response to unit step input

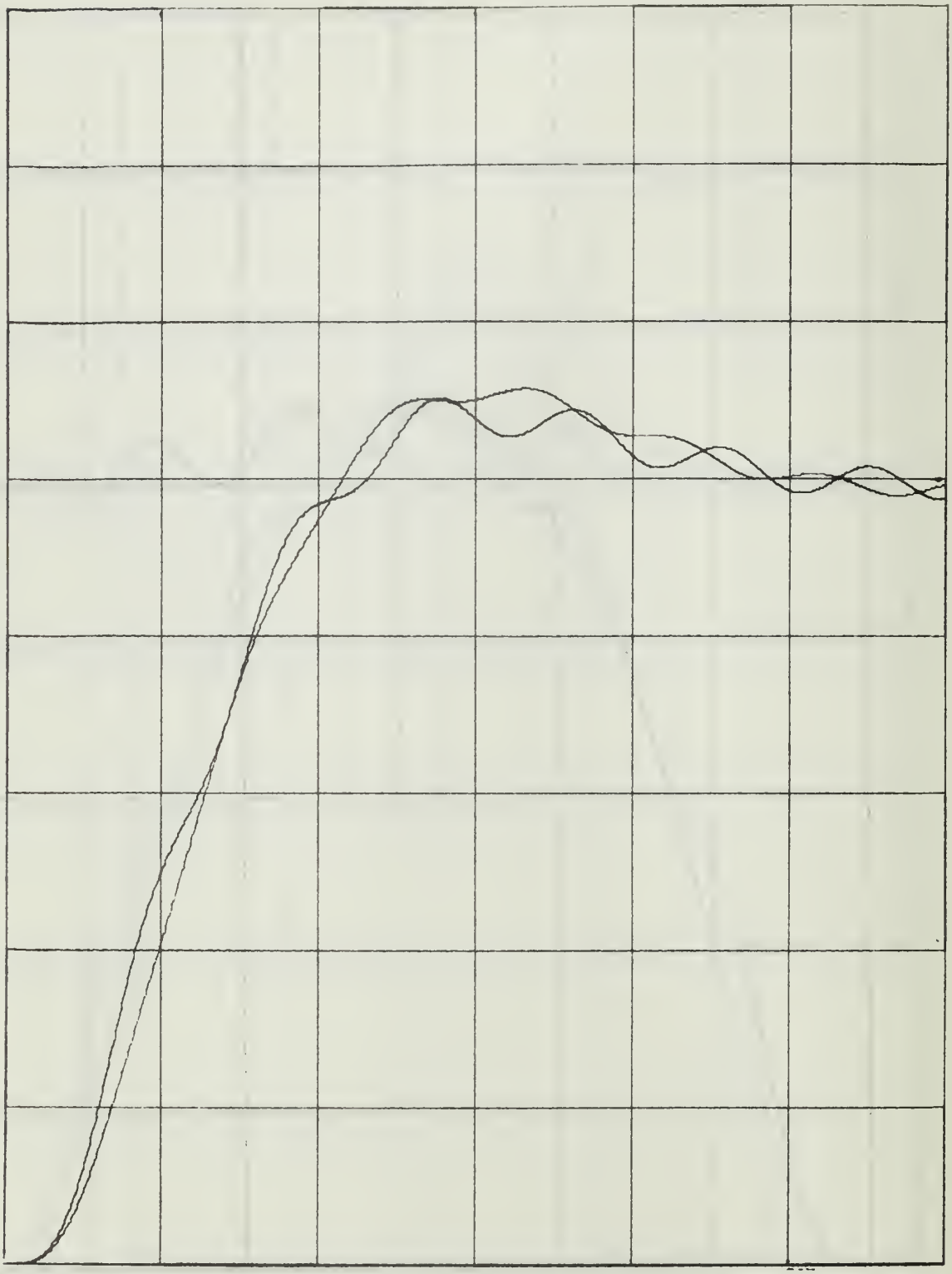

Figure A.16 Time response to unit step input

LIST OF REFERENCES

1. Franks, L. E. and Sandberg, I. W., "An Alternative Approach to the Realization of Network Transfer Functions: The N-Path Filter", The Bell System Technical Journal, p. 1321-1324, September 1960.

2. Astrionics Research and Development Report No. 3, Recent Developments in Adaptive Tracking Notch Filter Techniques, by M. T. Borelli, S. N. Caroll, and H. H. Hosenthien, p. 39-40, 1 March 1965.

INITIAL DISTRIBUTION LIST

		No. Copies
1.	Defense Documentation Center Cameron Station Alexandria, Virginia 22314	20
2.	Library Naval Postgraduate School Monterey, California 93940	2
3.	Dr. G. J. Thaler Department of Electrical Engineering Naval Postgraduate School Monterey, California 93940	5
4.	LCDR Tor R. Nilsen SFK/T 5070 Mathopen Norway	1
5.	Dr. W. J. McDaniel Department of Electrical Engineering Mississippi State University Drawer EE State College, Mississippi 39762	1
6.	Royal Norwegian Navy Bankplassen 2 Oslo Mil Oslo, Norway	1

Security Classification

DOCUMENT CONTROL DATA - R & D

(Security classification of title, body of abstract and indexing annotation must be entered when the overall report is classified)

1. ORIGINATING ACTIVITY (Corporate author)	2a. REPORT SECURITY CLASSIFICATION
Naval Postgraduate School Monterey, California 93940	Unclassified
	2b. GROUP

3. REPORT TITLE

Commutated Network Filter

4. DESCRIPTIVE NOTES (Type of report and inclusive dates)

Master's Thesis; December 1969

5. AUTHOR(S) (First name, middle initial, last name)

Tor Rønholt Nilsen

6. REPORT DATE	7a. TOTAL NO. OF PAGES	7b. NO. OF REFS
December 1969	55	2

8a. CONTRACT OR GRANT NO.	9a. ORIGINATOR'S REPORT NUMBER(S)
b. PROJECT NO.	
c.	9b. OTHER REPORT NO(S) (Any other numbers that may be assigned this report)
d.	

10. DISTRIBUTION STATEMENT

This document has been approved for public release and sale; its distribution is unlimited.

11. SUPPLEMENTARY NOTES	12. SPONSORING MILITARY ACTIVITY
	Naval Postgraduate School Monterey, California 93940

13. ABSTRACT

This thesis presents the results obtained in computer simulations of the commutated network filter. The commutated network filter is also used as a bandpass filter in servosystems. A linear approximation to the transfer function is found to be usable for design purposes.

DD FORM 1 NOV 65 1473 (PAGE 1)

S/N 0101-807-6811

Security Classification

A-31408

14 KEY WORDS	LINK A		LINK B		LINK C	
	ROLE	WT	ROLE	WT	ROLE	WT
Commutated network filter						
Bandpass filter						
Transfer function						
Frequency response						

thesN59
Commutated network filter.
3 2768 000 99631 8
DUDLEY KNOX LIBRARY